COX-2 Induction Suppresses Endothelial Inflammation Elicited by Lipoproteins and Low Shear Stress

By

EMILY MORENO
THESIS

Submitted in partial satisfaction of the requirements for the degree of

MASTER OF SCIENCE

in

Biomedical Engineering

in the

OFFICE OF GRADUATE STUDIES

of the

UNIVERSITY OF CALIFORNIA

DAVIS

Approved:

Anthony Passerini, Chair

Scott Simon

John Newman

Committee in Charge

2021

TABLE OF CONTENTS

LIST OF FIGURES

Introduction

Materials and Methods

Results

LIST OF ABBREVIATIONS

ASCVD – Atherosclerotic Cardiovascular Disease

NSAIDs – Non-steroidal anti-inflammatory drugs

EC – Endothelial Cells

HAEC – Human Aortic Endothelial Cells

TNFα – Tumor Necrosis Factor α

VCAM-1 – Vascular Cell Adhesion Molecule-1

ICAM-1 – Intercellular Cell Adhesion Molecule-1

ER – Endoplasmic Reticulum

BiP – Binding Immunoglobulin Protein

IRF-1 – Interferon Regulatory Factor-1

sXBP-1 – Spliced X-box Binding Protein-1

SS – Shear Stress

AOC – Artery-on-Chip

TGRL – Triglyceride Rich Lipoprotein

PUFA – Polyunsaturated fatty acids

COX – Cyclooxygenase

PDBu - Phorbol 12,13-dibutyrate

FBS – Fetal Bovine Serum

PBS – Phosphate Buffered Saline

PDMS – Polydimethylsiloxane

ABSTRACT

Atherosclerosis is a chronic inflammatory disease of arteries that leads to heart attack and stroke in over 3 million people per year in the US. The main risk factors for atherosclerotic cardiovascular disease (ASCVD) include dyslipidemia and disorders of metabolism. Moreover, there is a strong association between arterial flow characteristics and the local regulation of the inflammation that promotes ASCVD. Triglyceride rich lipoproteins (TGRL) are elevated in the circulation of individuals at risk for ASCVD and were shown to act synergistically with low magnitude shear stress (SS) to promote an inflammatory response by cultured human aortic endothelial cells (HAECs). This response was characterized by maximal vascular cell adhesion molecule (VCAM)-1 expression and was dependent upon an endoplasmic reticulum (ER) stress response. The magnitude of this response correlated strongly with enrichment in certain polyunsaturated fatty acid (PUFA) metabolites within the circulating lipoproteins that may be further metabolized by several enzymatic pathways in endothelial cells to produce an array of inflammatory mediators. We hypothesized that shifting endothelial cyclooxygenase (COX)-2-dependent PUFA metabolism alters the ER stress-mediated VCAM 1 upregulation in response to TGRLs.

TGRLs isolated from postprandial human plasma following a high fat test meal were characterized via flow cytometry as pro- or anti-inflammatory based on their impact on up- or down-regulation of VCAM-1 expression by HAEC relative to stimulation with tumor necrosis factor (TNF)α. TNFα stimulated HAEC monolayers were exposed to a SS gradient via artery-on-a-chip (AOC) microfluidics in the presence of TGRL and/or pharmacological intervention to induce or inhibit COX-2. ER stress markers that promote maximal VCAM-1 expression by TGRL in inflamed HAEC were analyzed by western blot. Despite a strong inverse correlation

between COX-2 and VCAM-1 expression observed in the SS gradient, the results did not strongly support a direct effect of COX-2 in mediating ER stress-induced VCAM-1 expression but implicated cross talk with other metabolic pathways. COX-2 expression was suppressed by low magnitude (atherosusceptible) SS and enhanced by high magnitude (atheroprotective) SS in the AOC device, registering a 37% increase from static control at 12 dynes/cm^2. COX-2 induction with phorbal-12,13-dibutyrate attenuated VCAM-1 across the SS gradient, reducing peak expression at 2 dynes/cm^2 by 62%. COX-2 upregulation by pharmacological induction or high magnitude SS suppressed ER stress-mediated VCAM-1 elicited by TNFα and TGRLs. These results are consistent with a protective role for COX- 2 in reducing endothelial inflammation that promotes atherosclerosis and reveal the potential for endothelial PUFA metabolism to modulate an inflammatory response to TGRL. Furthermore, a potent effect of low SS to enhance VCAM-1 expression while suppressing COX-2 expression was observed, consistent with its ability to promote an atherosusceptible phenotype, and demonstrating its importance when studying the inflammation promoting atherosclerosis.

INTRODUCTION

1.1 Atherosclerotic cardiovascular disease and its origins

Atherosclerosis is a chronic inflammatory disease of arteries that is the underlying cause of heart attack and stroke in over 3 million people per year in the US. Atherosclerotic cardiovascular disease (ASCVD) accounts for 1 in 3 deaths, making it the leading cause of death over cancer and chronic lower respiratory disease combined.[17] Atherosclerosis is characterized by plaque buildup along the inner artery walls, narrowing the lumen and ultimately obstructing blood flow. Plaque rupture and ensuing thrombosis may cause heart attacks and strokes.[17] Significant risk factors for ASCVD include dyslipidemia, diabetes, hypertension, smoking, and related changes in metabolism that promote inflammation. The risk for ASCVD can be reduced by maintaining a healthy diet and lifestyle and/or using medications, such as lipid lowering drugs (e.g., statins).[17]

Clinically, atherosclerotic dyslipidemia is characterized by elevated levels of ApoB-containing lipoproteins in circulation, including triglyceride-rich lipoproteins (TGRL). Elevated TGRL is a component of the metabolic syndrome, and particularly in the postprandial state, contributes to low-grade inflammation and associated endothelial dysfunction.[38] Epidemiological evidence links elevated TGRL with enhanced risk of ASCVD and mortality. We have previously reported on the mechanisms by which TGRL elicits the postprandial inflammatory responses that promote arterial inflammation.[2,19] Specifically, activation of an endoplasmic reticulum (ER) stress response mechanism culminates in activation of the transcription factor interferon

regulatory factor 1 (IRF-1), which modulates VCAM-1 expression in response to pro-inflammatory TGRL in human aortic endothelial cells (HAEC).[19]

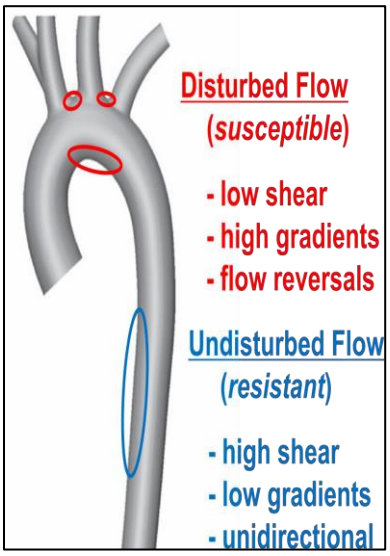

Figure 1.1.1: Sites of disturbed flow in arteries are susceptible to athero-inflammation

Regions of disturbed blood flow in arteries are more susceptible to the endothelial inflammation that promotes atherosclerosis. These atherosusceptible sites include bifurcations and curvatures that experience complex flow patterns, characterized in part by low magnitude time-averaged and oscillatory wall shear stress (figure 1.1.1). In contrast, more uniform vessel geometries experience relatively unidirectional flow and high magnitude shear stress considered atheroprotective.[4] The mechanosensitive arterial endothelium locally modulates inflammation in response to spatially varying wall shear stress (SS), which has been established as a key driver of endothelial phenotype and therefore an important context in which to study athero-inflammation. The mechanisms by which low shear stress promotes spatially varying vulnerability to atherosclerosis remain ill-defined, considering that ASCVD is exacerbated by a host of risk factors that are associated with metabolic dysregulation and systemic inflammation.

The atherosclerotic pro-inflammatory phenotype is associated with increased circulation of activated monocytes and pro-inflammatory cytokines. Two key atherogenesis biomarkers are an increase in VCAM-1 expression on the endothelial cell surface and VCAM-1-dependent monocyte recruitment.[2] VCAM-1 expression is an early marker of inflammation and is highly correlated to the development of atherosclerosis at sites of disturbed flow in arteries (i.e., low magnitude SS).[1,2,4] VCAM-1 serves as a counter receptor for very late antigen 4 (VLA-4) and

high-affinity integrin CD11c expressed on activated monocytes that is associated with increased monocyte arrest, trans-endothelial migration, and early onset of atherosclerosis.[32]

1.2 Artery-on-a-chip to measure endothelial inflammation

Because human arteries are not normally directly accessible to study the inflammatory mechanisms that promote atherosclerosis, the lab developed novel artery-on-a-chip (AOC) microfluidic tools that mimic essential attributes of sites susceptible to atherosclerosis, including low shear stress magnitudes and a spatially varying shear stress gradient. One AOC microfluidic design based on Hele-Shaw stagnation flow theory generates a linear shear stress gradient of 0-16 dynes/cm^2 over 20 mm (figure 1.2.1) over a monolayer of cultured endothelium.[1,23] The channel width (w) is a function of axial distance (x). L is the total channel length, w_1 is the entrance width, h is the channel height, μ is the viscosity of the flow medium, and Q is the volumetric flow rate; all these parameters are used to calculate the wall shear stress (τ_w) generated along the center line of the channel.[1] The flow channel thus models physiologically relevant arterial wall shear stress magnitudes ranging from those considered to promote atherosusceptibility to protective levels within a single experiment.

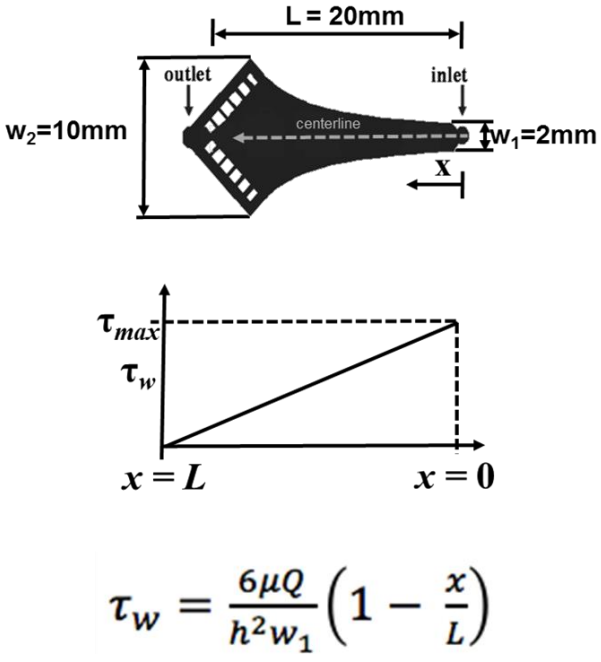

Figure 1.2.1: Hele-Shaw Artery-on-a-Chip channel design and dimensions. Wall shear stress equation calculated using viscosity of the flow medium, flow rate, and channel height, length, and entrance width.

This Hele-Shaw AOC allows us to directly visualize and reproducibly quantify VCAM-1, monocyte adhesion, and ER stress markers across the shear stress gradient in studies designed to elucidate mechanisms related to the regulation of athero-inflammation by shear stress.[1,33] High SS was found to reduce the inflammatory response on HAEC as reflected by VCAM-1 downregulation and a corresponding reduction in monocyte adhesion, while low SS exacerbated or was permissive to an inflammatory response in the AOC.[1] This device has enabled the ex vivo characterization of TGRL isolated from the serum of human subjects in terms of the capacity to promote early spatial and temporal inflammatory responses in endothelial cells and monocytes that are of functional relevance to ASCVD progression.

Using the AOC, we established that TGRL isolated from clinically healthy individuals after eating a standardized high saturated fat test meal, varied in its capacity to up- or down-modulate VCAM-1 expression by TNFα-stimulated HAEC. Pro-inflammatory VCAM-1 upregulation was signaled through an endoplasmic reticulum stress response that increased transcription factor interferon regulatory factor 1 (IRF-1) activity. Moreover, low magnitude SS (2 dynes/cm^2) was synergistic with TGRL and cytokine in eliciting maximal ER stress-mediated, IRF-1-dependent VCAM-1 expression. The VCAM-1 response measured in the AOC correlated strongly with a rise in recruitment efficiency monocytes.[24,25]

1.3 ER Stress-mediated inflammation

ER stress occurs when the ability of the ER to process proteins is overloaded, which promotes an increase in ER membrane expansion and activation of the unfolded protein response (UPR), leading to restored equilibrium or cell death. The UPR constitutes a set of signaling

pathways that help maintain normal cellular homeostasis and plays a role in atherosclerosis.18 ER stress and activation of the UPR modulates VCAM-1 expression as a function of the relative atherogenicity of TGRL.3 Figure 1.3.1 illustrates the major ER stress response pathways. 4-phenyl butyric acid (4-PBA), an ER stress inhibitor, significantly downregulated VCAM-1 expression by inflamed HAEC. HAEC treated with pro-atherogenic TGRL revealed an increase in membrane expansion and ER stress, and further upregulated VCAM-1 expression that was abrogated by treatment with 4-PBA. Low magnitude SS applied to HAEC activates the splicing of x-box binding protein 1 (XBP-1) to produce its active form spliced XBP-1 (sXBP-1) and eukaryotic initiation factor 2α (eIF2α).[4] sXBP-1 and eIF2α then differentially regulate interferon regulatory factor-1 (IRF-1) activity, which serves as a link between TGRL metabolism and inflammatory regulation of VCAM-1.[3,4] As a transcription factor sensitive to both shear stress and TGRL, IRF-1 could be a potential drug target for mediating athero-inflammation.

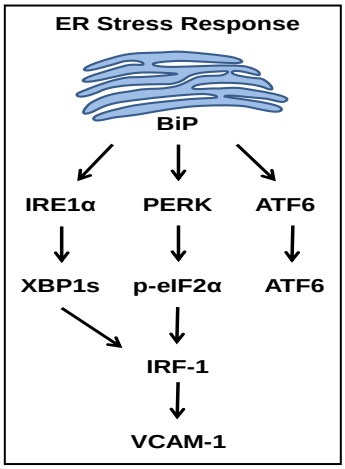

Figure 1.3.1: The three arms of the ER stress-induced unfolded protein response.

1.4 TGRL composition and inflammation

A high fat diet exacerbates inflammation by increasing dietary lipoproteins and cytokines in circulation.[3] Triglyceride-rich lipoproteins (TGRL) are lipid-rich protein carriers that when elevated represent a causal risk factor for low-grade inflammation and ultimately ASCVD.[28] TGRL composition is unique for each individual and is dependent on the administered meal content, the postprandial state vs fasting state, and an individual's overall metabolism. Circulating TGRL can modify the endothelial inflammatory response depending on an

individual's unique composition, but this inflammatory response is subjected to further spatial modulation by shear stress. TGRL elevated postprandially by individuals with metabolic dysregulation, act synergistically with low magnitude SS to promote an inflammatory response by cultured HAEC.[2] The magnitude of this response correlates strongly with enrichment in the non-esterified polyunsaturated fatty acid (PUFA) metabolites within the circulating lipoproteins.[7] We have observed that the inflammatory response to an individual's unique TGRL correlates with markers of metabolic dysregulation (e.g. waist circumference, hypertriglyceridemia).[9,19] Moreover, pro-inflammatory responses in HAEC were observed postprandially as opposed to in the fasting state.

Differences in TGRL composition correlate with the variable inflammatory response to a standard high fat meal observed across individuals. Using an unbiased metabolomics analysis, it was determined that TGRL from dyslipidemic subjects eliciting a pro-atherogenic response assessed in the AOC were most strongly enriched in non-esterified polyunsaturated fatty acids (PUFA) and their metabolites (oxylipins).[7] This study identified a signature of oxylipins transported in TGRL that reflected an individual's metabolism and strongly correlated with an endothelial-mediated pro-atherogenic response. However, whether enrichment in specific oxylipins in TGRL is causative in promoting athero-inflammation, and how this might be further regulated by the endothelium in the context of physiological SS is unknown.

Bioactive lipids produced from metabolism of PUFA function as messengers that regulate cell behavior, including inflammation. PUFA circulating in TGRL may be significant because, although present at relatively low abundance, PUFA may be metabolized by enzymes in endothelial cells to produce oxylipins, bioactive mediators that regulate inflammatory responses. PUFAs in TGRL are metabolized via three enzymatic pathways: cyclooxygenases (COX), lipoxygenases (LOX), and cytochrome P450s/soluble epoxide hydrolase (CYP/sEH). The products of these metabolic enzymes in HAEC can be either pro-inflammatory or anti-inflammatory, as denoted by red and blue, respectively. However, it was recently discovered that prostaglandin D_2 has demonstrated anti-inflammatory effects in addition to pro-inflammatory actions.[43] Therefore these pro- vs anti-inflammatory distinctions may be over-generalized and there may be a contextual aspect to the specific nature of the regulatory impact of this and other members of the described cascades. Diols are formed by sEH and have been shown to have a neutral or pro-inflammatory effect on inflammation[34] (figure 1.4.1). The oxylipin composition circulating in lipoproteins varies in response to diet and intervention.[3,4] Enrichment in the non-esterified PUFA within postprandial TGRL, including the products of sEH metabolism, correlated with a pro-atherogenic increase in VCAM-1 expression by HAEC. Understanding how PUFA transported within TGRL are further metabolized upon uptake by endothelium to produce an array of

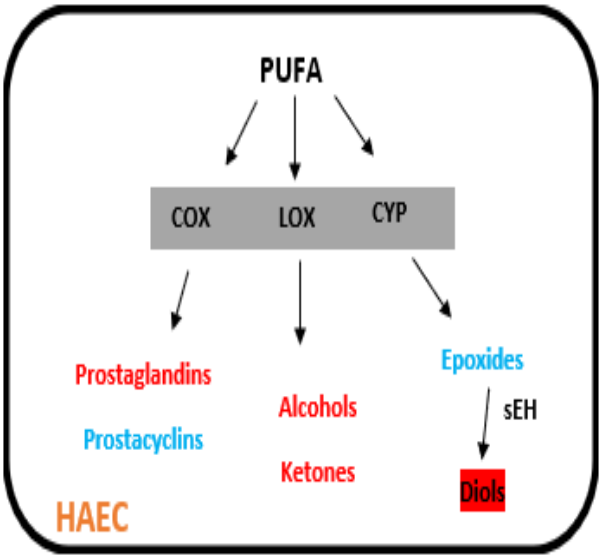

Figure 1.4.1: PUFA metabolism pathways and the canonical effects on inflammation.

oxylipins is an important step toward elucidating the mechanisms that regulate athero-inflammation. Furthermore, shear stress may exert additional effects on endothelial PUFA metabolism to promote a susceptible or protective phenotype, in the presence of TGRL of differing composition.

1.5 Role of COX-2 in endothelial inflammation

COXs are known to play an important role in the regulation of inflammation.[16] COX-1 is constitutively expressed in endothelial cells, while COX-2 is induced by cytokines, growth factors, and laminar SS.[9] COX-2 is localized in the nucleus, while COX-1 is present in the cytoplasm.[26] The COXs are best known for their role in the production of prostanoids derived from arachidonic acid (AA) through a two-step process, though they may act on other PUFA as well. Prostaglandin I_2 (PGI_2, prostacyclin) is a vasodilator and an anti-atherogenic prostanoid produced in EC, first by the conversion of AA to prostaglandin H_2 (PGH_2) through the activation of COX isoenzymes, then by prostacyclin synthase to produce PGI_2.[10,14,16] PGI_2 counteracts the effects of other pro-inflammatory and pro-thrombotic COX metabolites such as PGE_2 and thromboxane (TXA_2), derived from platelets and activated macrophages, in the regulation of vascular homeostasis.[12,16] COX-2 plays a protective role in reducing endothelial inflammation that promotes atherosclerosis.[22] In hyperlipidemic mouse models, global deletion of COX-2 accelerated atherosclerosis. Selective COX-2 deletion in vascular endothelial and smooth muscle cells resulted in suppression of PGI_2, increased blood pressure, and increased atherosclerotic burden.[12] Inhibition of COX-2-derived PGI_2, e.g., through selective non-steroidal anti-inflammatory drugs (NSAIDs), can lead to increased risk of serious cardiovascular consequences by removing a suppressive effect on thrombosis, hypertension, and atherosclerosis.[6, 12, 16]

In contrast to COX-1, COX-2 expression and activity are known to be upregulated by athero-protective SS.[20] COX-2 is induced by an inflammatory challenge and by increasing shear stress magnitude, further suggesting its role in spatial regulation of the inflammation promoting atherosclerosis.[28,29] Subsequent studies in HUVEC revealed that COX-2, but not COX-1, mRNA expression rapidly increased under laminar SS > 5 dynes/cm^2 and was sustained with SS at 24 hr. Upregulation of the COX-2 protein was also observed.[20,13] More recently a mechanotransduction mechanism involving PECAM-1, focal adhesion kinase, and $\alpha_5\beta_1$ integrin was reported to signal the sustained expression of COX-2 and production of PGI_2 by athero-protective SS in BAEC and HUVEC.[10] Further supporting a suppressive effect of COX-2 on athero-inflammation, EC treated with the COX-2 selective inhibitor rofecoxib displayed an increase in monocyte adhesion, implicating upregulation of VCAM-1.[11]

The role of the COX pathways in regulating the endothelial inflammatory response to the multitude of fatty acids and their metabolites circulating in the lipoproteins of dyslipidemic individuals, particularly in the context of physiologically relevant shear stresses, has not been studied. Our preliminary data presented herein revealed that COX-2 induction was sufficient to shift the HAEC response to TGRL from pro- to anti-atherogenic, motivating the focus of this thesis on this particular metabolic pathway.

1.6 Thesis objectives

The main objective of this work was to determine how endothelial PUFA metabolism by COX-2 regulates an inflammatory response to TGRL in the context of shear stresses that promote susceptibility to or resistance to atherosclerosis. Our hypothesis was that shifting

endothelial PUFA metabolism through modulation of the COX-2 pathway alters the ER stress-mediated VCAM-1 upregulation elicited by pro-inflammatory TGRL. Due to its athero-protective tendencies, we hypothesized that COX-2 induction suppresses ER stress-mediated VCAM-1 expression elicited by lipoproteins and low shear stress. By manipulating the COX-2 pathway and altering endothelial PUFA metabolism, we propose to shift the inflammatory phenotype of HAEC and elucidate the role of ER-stress mediated VCAM-1 regulation. This study is expected to enhance our understanding of the mechanisms that link dyslipidemia, metabolism, and endothelial mechanobiology in the regulation of the inflammation promoting atherosclerosis.

MATERIALS AND METHODS

2.1 Cell culture

Human aortic endothelial cells (Genlantis; lot #7F4409 from a 34-year-old male) were used for these experiments at passages 5-7 (<15 population doublings), in their rapid growth phase. HAEC were cultured in endothelial cell growth medium, which consisted of basal medium supplemented with 1X Antibiotic-Antimycotic (Gibco; #15240062) and supplement mix (PromoCell; C-22010). The supplement mix contained fetal calf serum, endothelial cell growth supplement, epidermal growth factor, basic fibroblast growth factor, heparin, and hydrocortisone. To induce a consistent acute inflammatory response, cells were stimulated with TNFα at the EC_{50} for VCAM-1 and ICAM-1 upregulation, calculated from TNFα dose response curves by flow cytometry. Some experiments used TNFα from a lot for which the EC_{50} was 0.3 ng/ml TNFα (R&D systems; #210-TA-100/CF; lot DDHB0114112 (20 ug)), while others used 0.6 ng/ml TNFα (R&D systems; #210-TA-100/CF; lot DDHB0320021 (100 ug)) calculated for a different lot. Stimulation at the EC_{50} served as an internal control for each experiment.

2.2 COX-2 siRNA transfection

COX-2 siRNA transfection using lipofectamine RNAiMAX (Thermo Fisher; #13778030) was used to knockdown COX-2 expression in HAEC. Cells were seeded in 6 well plates at 130,000 cells per well in serum free endothelial growth medium. 24 h after seeding, lipofectamine and 80 pmol of COX-2 siRNA (Santa Cruz Biotechnology; #sc-29279) or control siRNA (Santa Cruz Biotechnology, #sc-37007) were diluted in Opti-MEM transfection medium (Thermo Fisher,

#31985062) and added to each well. Plates were then incubated at 37 C for 24 h. COX-2 knockdown efficiency of 87% was confirmed by western blot analysis.

2.3 COX-2 pharmacological intervention

Pharmacological inducers and inhibitors were used to modulate the COX-2 enzyme to investigate the downstream effects on PUFA metabolism and HAEC inflammatory response. HAEC were pre-incubated with COX-2 inducer, phorbol-12,13-dibutyrate (PDBu, 1 uM), or COX-2 inhibitor, rofecoxib (1 uM), for 1 h. They were then incubated with TNFα and/or TGRL (10 mg/dl ApoB) for western blot, flow cytometry, and microfluidic experiments.

2.4 Human subject participation

Human subjects were recruited according to a UC Davis Institutional Review Board approved protocol (#219114) to study lipoprotein interaction with the vascular endothelium and provided informed consent. Participants were screened against the exclusion criteria, which included a history of cardiovascular, liver, or kidney disease, untreated thyroid dysfunction, use of lipid lowering medication, hormone replacement therapy, regular NSAID use, pregnancy, weight < 123 pounds, and dietary restrictions (e.g., vegan). Eligible participants fasted for 12 h before a fasting blood draw. One 3.5 mL BD SST serum separator vacutainer tube (Beckton and Dickenson, Franklin Lakes, NJ) was collected for a standard lipid panel, one 4 mL tube was collected for assessment of blood glucose, and six 8 mL BD PST plasma separation/lithium heparin tubes were collected for TGRL isolation. The tubes were centrifuged for 10 min at 1344 rcf (2800 rpm) at 25 ºC to separate the plasma. Immediately after the fasting blood draw,

participants consumed a high fat breakfast meal in under 30 min. The high fat breakfast meal consisted of 2 McDonald's sausage McMuffin with egg sandwiches, 1 hashbrown, and a small 12 oz Minute Maid orange juice. It was composed of a total of 1250 calories, 25 g saturated fat, 114 g carbohydrates, 44 g protein, 1 g trans-fat, 36 g total sugars, 560 mg cholesterol, 7 g dietary fiber, and 2005 mg sodium. 3.5 h after consuming the meal, a postprandial blood draw was performed to collect additional samples for preprocessing and analysis as described above.

2.5 TGRL isolation and characterization

Fasting and postprandial plasma from the PST plasma separation/lithium heparin tubes was collected and pooled for each subject. 1X Antibiotic-Antimycotic was added to each plasma container. The plasma samples were then aliquoted and balanced for ultracentrifugation in mock buffer for 18 h at 274355 rcf (40,000 rpm) at 4 ºC to isolate TGRL from plasma using an Optima LE-80K Centrifuge. Isolated fasting and postprandial TGRL (density < 1.0063 g/mL) were collected and aliquoted. Fresh TGRL not used for experiments within a week of isolation were flushed with nitrogen gas to reduce oxidation and stored at -80 ºC. A human ApoB ELISA assay kit (Assaypro; #EA7001-1) was used to quantify the ApoB content in the TGRL samples. The TGRL volume was normalized to 10 mg/dL ApoB for characterization via flow cytometry as described below. The percent change in VCAM-1 from the control (TNFα EC_{50}) response was used to determine if the TGRL elicited a pro- or anti-inflammatory response in HAEC. VCAM-1 percent change values of >10% from the control were considered pro-inflammatory, <-10% anti-inflammatory, and -10% <x <10% neutral.

2.6 Flow cytometry

HAEC were seeded at 65-100 thousand cells per well in 12-well tissue culture plates and grown to 85-95% confluency. They were then incubated in growth media, 8% FBS (Thermo Fisher Scientific; #16000036), and stimulated at the EC_{50} for TNFα-induced CAM expression (R&D systems; #210-TA-100/CF) as determine through a dose response curve, for 4 h at 37 ºC. For experiments using TGRL, 10 mg/dL ApoB was used per well to normalize the number of lipoprotein particles. For experiments using PDBu and/or rofecoxib, cells were pre-treated (1 μM) for 1 h before the 4 h incubation. Cells were then dissociated after 4 h using 1 mM EDTA (Sigma; #T9285) for 15 min, collected in 2 mL Eppendorf tubes and spun down at 500 rcf, 4 ºC for 3 min. Cells were stained with phycoerythrin-conjugated VCAM-1 antibody (BD Biosciences; #555647; 10 μL per 100,000 cells) and Alexafluor 488-conjugated (ICAM-1) antibody (Biolegend; #322714; 5 μL per 100,000 cells) for 45 min. Cells were suspended in cell staining buffer (Biolegend; #420201) and centrifuged under the same settings. Cells were then re-suspended in cell staining buffer and VCAM-1 and ICAM-1 surface expression were measured using flow cytometry (Attune NXT). The Attune NXT parameter settings were forward scatter – 75 V, side scatter – 125 V, BL1 – 250 V, and YL1 – 320 V.

2.7 Western blots

HAEC were seeded at 120-300 thousand cells per well in 6-well tissue culture plates and grown to 90-95% confluency. They were then incubated in growth media, 8% FBS, and TNFα (EC_{50} for CAM upregulation) (R&D systems; #210-TA-100/CF) for 4 hours at 37 C. For experiments using TGRL, treatments were normalized to 10 mg/dL ApoB. For experiments using PDBu

and/or rofecoxib, cells were pre-treated (1 μM) for 1 h before the 4 h incubation. Cells were scraped and lysed using RIPA buffer (Millipore Sigma; R0278-50ML) and protease inhibitor cocktail (Millipore Sigma; P8340) after the 4 h incubation period. Cell lysates were stored at -20 ºC. 4X Laemmli sample buffer (Bio-Rad; #1610747) and 2-mercaptoethanol (Bio-Rad; #1610710) were added to cell lysates that were then denatured on a hot plate at 95 ºC for 6 min. Depending on the proteins of interest, samples were loaded into 6-12% lower Bis-Tris acrylamide gels and run at 80 V for 20 min, incrementing by 20 V every 20 min (200 V max) until an ideal protein separation was reached. The proteins were transferred to nitrocellulose membranes (Bio-Rad; #1620094) at 100 V for 2 h on ice. Membranes were then submerged in ponceau stain for 1 min to verify a successful transfer. Membranes were then cut into strips depending on proteins of interest and blocked overnight in 5% milk in TBST. The next day membranes were incubated with the following primary antibodies in 2% milk in TBST for 2 h: COX-2 Rabbit mAb (Cell Signaling Technology; #12282; 1:1,000 dilution), COX-1 Rabbit mAb (Cell Signaling Technology; #9896; 1:1,000 dilution), total IRE1α Rabbit mAb (Cell Signaling Technology; #3294; 1:1,000 dilution), p-IRE1α [p Ser724] (Novus; #NB100-2323SS; 1:1,000 dilution), anti-GRP78 BiP (Abcam; #21685; 1:500 dilution), XBP-1s Rabbit mAb (Cell Signaling Technology; #40435; 1:1,000 dilution), purified anti-IRF-1 (Biolegend; #657602; 1:500 dilution), and GAPDH (Novus; #NB300-328; 1:10,000 dilution) which served as the loading control. Membranes were washed in TBST and incubated with their following respective secondary antibody for 1 h: peroxidase goat anti-rabbit IgG (Jackson Immuno Research Laboratories; #111-035-003; 1:2,000 dilution) or peroxidase goat anti-mouse IgG (Jackson Immuno Research Laboratories; #115-035-003; 1:2,000 dilution). After washing, membranes were incubated in West Femto chemiluminescent substrate (Thermo Fisher Scientific; #34095)

or West Pico chemiluminescent substrate (Thermo Fisher Scientific; #34580) for 5 min and imaged using the ChemiDoc (Bio-Rad).

2.8 Microfabrication

Hele-Shaw stagnation flow theory informed the design of the microfluidic polydimethylsiloxane (PDMS) chips mimicking arterial flow with wall shear stress values of 0-16 dynes/cm^2.[1] The Hele-Shaw based microfluidic chamber was designed in SolidWorks and fabricated using soft photolithography. From the 2D design, a 5x7 photomask was printed at 5000 dpi (CAD/Art Services). Silicon wafers 100 mm wide and 500 µm thick (University Wafer; #452) were cleaned in piranha solution (50/50, 95-98% sulfuric acid and 30% hydrogen peroxide) for 20 min. The wafer was suctioned to a spin coater and SU-8 2050 photoresist was poured over the wafer and spun at 288 rcf (1700 rpm) for 40 sec to create a 100-µm thick photoresist layer. The photomask was then aligned over the wafer and exposed to a UV light for 1 min and baked at 65 ºC for 2 min, 95 ºC for 7 min, and 180 ºC for 10 min to harden the layer, thus creating the master. To create the PDMS chamber, the master wafer was placed inside a petri dish and filled with a 1:10 ratio of 184 curing agent to silicon elastomer base mixture (Krayden; #DC4019862) to a height of 1 cm. The dish was degassed and baked at 70 ºC for 3 h. A blade was used to remove the chambers from the mold and a 19-gauge needle was punched into the chip to create the inlet, outlet, and vacuum holes.[23] The Hele-Shaw channel was later optimized in SolidWorks to create a longer entrance region for flow to fully develop and increase cell yield in the 12 dynes/cm^2 region. Specifically, the entrance length was extended by 3 mm and kept at a width of 2 mm, extending the 16 dynes/cm^2 region by 3 mm. Figure 2.8.1 displays the revised CAD sketch of the chamber and representative images at 12 dynes/cm^2 using the original chip and the new extended

entrance chip. The images demonstrate that cell yield increased at an essential shear stress magnitude using the new chip, making it easier to gather more data points at high shear stress magnitudes.

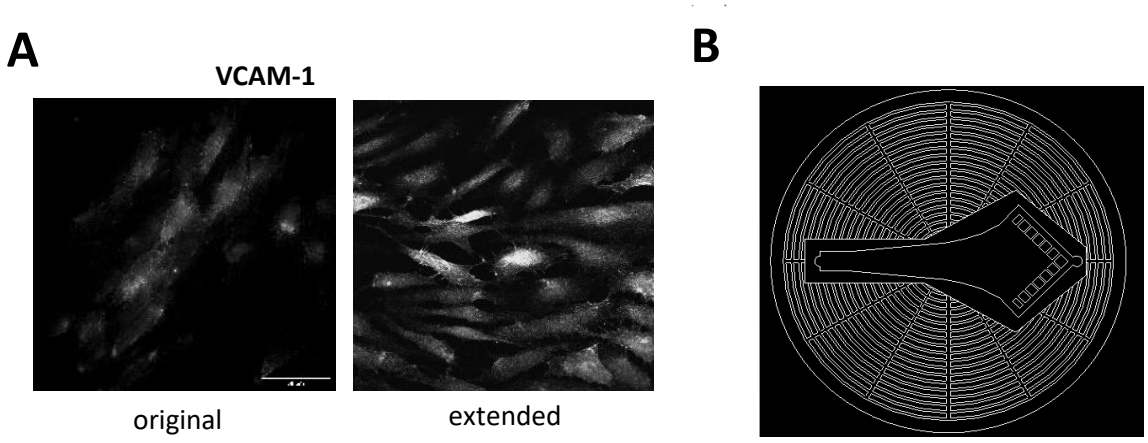

Figure 2.8.1: (A) Representative images of VCAM-1 expression after a 4 h AOC flow run at 12 dynes/cm^2 using the original chip and new extended chip. HAEC were imaged by confocal microscopy. (B) 2D CAD sketch of the extended microfluidic chamber.

2.9 Artery-on-a-chip (AOC) microfluidics

HAEC were seeded on collagen (Thermo Fisher Scientific; #A1048301; 100 ug/ml) coated 35 mm diameter glass slides and grown to 90-95% confluency for AOC experiments. Each monolayer of HAEC on the glass cover slip was adhered to a PDMS chip via a vacuum network system. The assembly was then connected in a closed loop flow system with a peristaltic pump driving media flow through the Hele-Shaw channel. The entire flow loop was enclosed in a chamber maintained at 37 ºC. A flow rate was established that produced a linear shear stress gradient of 0-16 dynes/cm^2 across the channel. The medium circulating through the system consisted of Leibovitz-15 medium (Gibco; #11415-064) supplemented with EGM-2 Endothelial SingleQuots (Lonza; CC-4176), 8% FBS, 1X Antibiotic-Antimycotic, and TNFα (EC_{50}). TGRL (10 mg/dL ApoB), PDBu (1 µM), and rofecoxib (1 µM) were also added to the medium for some

experiments. AOC flow runs were 2 h long when targeting peak IRF-1 and sXBP-1 expression, and 4 h long for VCAM-1and ICAM-1 peak expression. After the flow run time, HAEC monolayers were observed under the microscope to ensure the cells remained present and at consistent density from the inlet to the outlet (16-0 dynes/cm^2). The HAEC were then fixed in 4% paraformaldehyde (Electron Microscopy Sciences; #15710) for 10 min and stored at 4 ºC for up to a week before immunofluorescence staining.

2.10 Immunofluorescence staining and confocal microscopy

Fixed, sheared HAEC from AOC flow runs were blocked in buffer containing PBS with calcium and magnesium (Thermo Fisher Scientific, #14040133) supplemented with 2% TruStain FcX (Biolegend; #422301) and 0.1% Triton X-100 (Millipore Sigma; #21123) for 1 h at room temperature. After the hour, HAEC were incubated with the following primary antibodies diluted in blocking buffer overnight at 4 ºC: phycoerythrin-conjugated VCAM-1 antibody (BD Biosciences; #555647; 1:10 dilution), Alexafluor 488-conjugated (ICAM-1) antibody (Biolegend; #322714; 1:20 dilution), purified anti-IRF-1 (Biolegend; #657602; 1:100 dilution), XBP-1s Rabbit mAb (Cell Signaling Technology; #40435; 1:200 dilution), COX-2 Rabbit mAb (Cell Signaling Technology; #12282; 1:200 dilution), and COX-1 Rabbit mAb (Cell Signaling Technology; #9896; 1:200 dilution). The next day, HAEC were incubated with the following respective secondary antibodies diluted in blocking buffer for 1 h at room temperature: goat anti-rabbit IgG Alexa Fluor 647 (Thermo Fisher Scientific; #A21245: 1:500 dilution) and goat anti-mouse IgG Alexa Fluor 555 (Thermo Fisher Scientific; #A21425: 1:500 dilution). The glass cover slips were then mounted on microscope slides using ProLong Diamond Antifade Mountant with DAPI (Thermo Fisher Scientific; #P36962). Slides were imaged on an Olympus FV3000

laser scanning confocal microscope using lasers 405, 561, and 640. 3-6 representative images (~60 cells average) from each slide (n =3-5) were taken at axial positions corresponding to the following shear stress magnitudes: 0, 2, 4, 6, 8, 10, 12 dynes/cm^2. Mean fluorescence intensity was measured for each cell. The average mean fluorescence intensity at each shear stress magnitude was calculated for each slide. Those averages were then reported relative to the TNFα static (0 dynes/cm^2) to generate % change from static values.

2.11 Image processing

Western blot ChemiDoc files were analyzed using ImageJ FIJI analysis software. Proteins were normalized to the loading control, GAPDH. Confocal image files of AOC experiments were also analyzed using ImageJ FIJI analysis software. DAPI staining was used to identify HAEC. Fiji scripts using thresholding were used to quantify nuclear staining (sXBP-1, IRF-1), cytoplasmic staining (COX-2), and whole cell (VCAM-1). The mean fluorescence intensity of the targets was measured for each cell at 0, 2, 4, 6, 8, 10, 12 dynes/cm^2. The average at each of these magnitudes was taken for every stained sample (n =3-5) and used to calculate the % change from static (0 dynes/cm^2). The % change values of the mean fluorescence intensity were then plotted for 2-12 dynes/cm^2.

2.12 Data analysis

All experimental quantitative data were analyzed using GraphPad Prism 9 (Graphpad Software Inc, San Diego, CA). All the experimental data sets had at least n =3 per experimental group or condition. ANOVA and Dunnett's multiple comparisons tests were used to compare shear stress

values 2, 4, 6, 8, 10, and 12 dynes/cm^2 to the static control (0 dynes/cm^2) for flow data. It was also used to compare COX-2 induction and inhibition via pharmacological intervention to the DMSO control. ANOVA and Sidak's multiple comparisons tests were used to compare the difference of a condition between 2 experimental groups for flow cytometry and western blot data. T-tests were performed to analyze differences between 2 experimental groups. P-values were calculated and considered significant for 2-tailed $p < 0.05$, unless otherwise specified.

RESULTS

3.1 Shear stress elicits a variable COX-2 response to TNFα stimulation

When performing AOC flow experiments, stimulation of HAEC at the EC_{50} for CAM upregulation by TNFα is necessary to elicit a consistent VCAM-1 response that varies reproducibly across the shear stress gradient from 0-16 dynes/cm^2. These results are seen in figure 3.1.1. The TNFα static mean fluorescence intensity (observed at the stagnation point in the Hele-Shaw device, 0 dynes/cm^2) serves as an internal control for each experiment from which to calculate relative changes at each shear stress level. To determine how COX-2 expression by HAEC varied as a function of inflammatory stimulation and SS, monolayers were exposed to the SS gradient in the Hele-Shaw AOC for 4 h in the presence and absence of TNFα and results are shown in figure 3.1.1. As was the case with VCAM-1 expression, COX-2 was expressed at low levels in unstimulated HAEC, indistinguishable from background binding of isotype control antibodies, and did not differ significantly with shear stress. When comparing the VCAM-1 in the presence or absence of TNFα, there is a significant difference between the two at the low shear stress magnitudes, peaking at 2 dynes/cm^2 where VCAM-1 displays maximal expression. In contrast, the change in TNFα-induced COX-2 expression is significant at high shear stresses, peaking at 12 dynes/cm^2. These results demonstrate that TNFα (EC_{50}) stimulation is necessary to elicit significant change in VCAM-1 and COX-2 expression which varied as a function of shear stress.

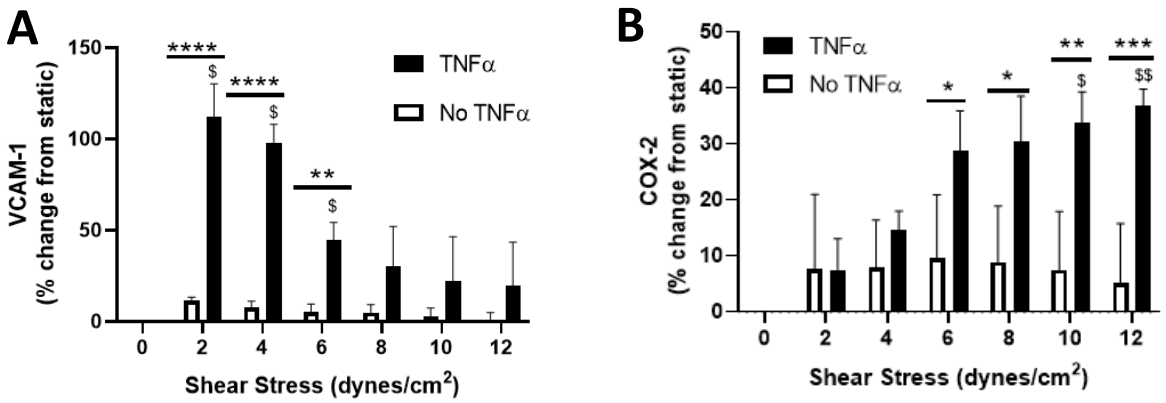

*Figure 3.1.1: VCAM-1 (A) and COX-2 (B) expression after a 4 h AOC flow run in the presence and absence of TNFα (EC_{50} for CAM upregulation) across a shear stress gradient of 0-12 dynes/cm^2. HAEC were imaged by confocal microscopy. Values are means ± SD. *p <0.05, **p <0.001, ***p <0.0005, **** p < 0.0001 between TNFα vs no TNFα.$ p <0.05, $$ p <0.01 represents significant changes in expression when compared to the static control. n =5 slides.*

Figure 3.1.1 also demonstrates the shear stress magnitudes that differ significantly from static (0 dynes/cm^2) for VCAM-1 and COX-2 expression in the presence of TNFα during a 4 h AOC flow run as denoted by the '$' symbol. VCAM-1 expression significantly increased and peaked at 2 dynes/cm^2, which has been observed in previous studies. COX-2 expression displayed an increasing trend with shear stress magnitude and was significantly increased at 10 and 12 dynes/cm^2 when compared to the static control. Thus, these proteins displayed an inverse pattern of regulation in response to shear stress magnitude within the same endothelial monolayers. Figure 3.1.2 illustrates a simple linear regression analysis with an R^2 value of 0.9834, slope of -3.45, and a p-value of 0.0001 for the TNFα data. This further demonstrates the significant inverse correlation between COX-2 and VCAM-1 in HAEC across the shear stress gradient when stimulated with TNFα.

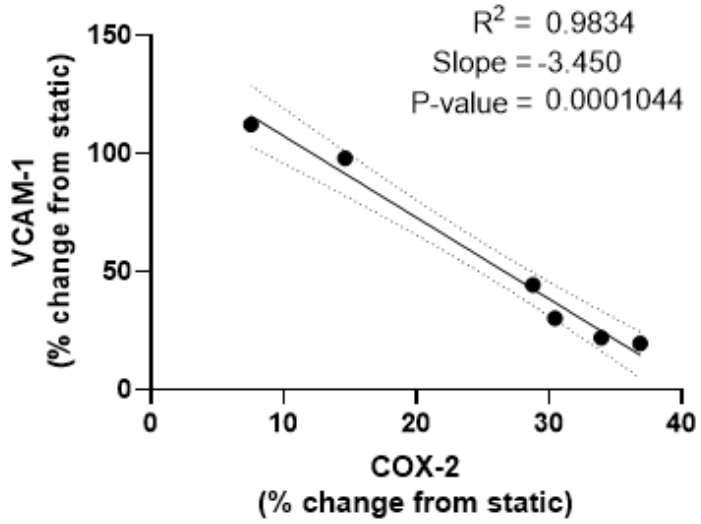

*Figure 3.1.2: Simple linear regression analysis showing the inverse correlation between COX-2 and VCAM-1 in HAEC stimulated with TNFα. VCAM-1and COX-2 expression after a 4 h AOC flow run in the presence of TNFα (EC_{50} for CAM upregulation) across a shear stress gradient of 0-12 dynes/cm^2. HAEC were imaged by confocal microscopy. Values are means ± SD. ***p <0.0005 correlation. n =5 slides.*

3.2 Characterization of human subjects

TGRL isolated postprandially from human plasma, as detailed in the IRB-approved meal study outlined in the methods, was used for experiments to investigate its role in ER stress-mediated VCAM-1 regulation in HAEC. TGRL eliciting both pro- and anti-inflammatory responses were used for experiments, defined by the relative effect on endothelial CAM expression. The donor non-metabolic characteristics and their TGRL CAM-responses are stratified by pro- and anti-inflammatory TGRL phenotypes in table 3.2.1. TGRL from 23 donors (M =13, F =10) were used. On average, the pro-inflammatory TGRL increased VCAM-1 expression by 36%, while the anti-inflammatory decreased it by 32%. There were no significant differences between the groups with respect to age, BMI, waist to hip ratio (WHR), or waist circumference.

Table 3.2.1: Non-metabolic characteristics of subjects grouped by their inflammatory response to TGRL. Values are means ± SD.

VCAM-1 (% change)	ICAM-1 (% change)	Age (years)	Gender (M/F)	BMI (kg/m^2)	Waist: Hip	Waist Circumference (cm)
Pro-inflammatory (n =16)						
35.9 ± 25.9	24.5 ± 22.5	38.5 ± 14.6	7/9	26.6 ± 3.6	0.89 ± 0.09	87.1 ± 10.8
Anti-inflammatory (n =7)						
-32.4 ± 11.5	-10.8 ± 26.4	33.0 ± 16.6	6/1	24.1 ± 2.7	0.96 ± 0.03	85.2 ± 8.5

Lipid and metabolic panel results from donors characterized as pro- or anti-inflammatory by their response to TGRL are shown in table 3.2.2 and table 3.2.3, respectively. A Mann-Whitney t-test (non-parametric) was used to analyze the difference between the fasting and postprandial results from both subsets. There was a significant increase in TG postprandially in both pro- and anti-inflammatory donors. There were no significant differences between the pro- and anti-inflammatory postprandial TGRL with respect to TG or HDL.

Table 3.2.2: Lipid and metabolic panels from subjects with pro-inflammatory TGRL. Values are means ± SD. P-values calculated by Mann-Whitney t-test.

Pro-inflammatory (n =16)	**Fasting**	**Postprandial**	**p-value**
Non-HDL TC (mg/dl)	162.4 ± 107.3	164.9 ± 96.2	0.6139
TC (mg/dl)	214.0 ± 101.4	213.6 ± 89.6	0.8500
HDL (mg/dl)	51.6 ± 13.8	48.7 ± 14.3	0.4555
LDL (mg/dl)	143.7 ± 106.7	191.0 ± 152.8	0.9451
TC: HDL	4.7 ± 3.8	5.1 ± 4.0	0.3539
TG (mg/dl)	105.2 ± 68.5	271.6 ± 171.1	***0.0007
Glucose (mg/dl)	84.4 ± 8.4	78.2 ± 11.5	0.1723
Apolipoprotein B-100 (mg/dl)	105.6 ± 65.5	98.9 ± 52.2	0.7790

Table 3.2.3: Lipid and metabolic panels from subjects with anti-inflammatory TGRL. Values are means ± SD. P-values calculated by Mann-Whitney t-test.

Anti-inflammatory (n =7)	**Fasting**	**Postprandial**	**p-value**
Non-HDL TC (mg/dl)	130.3 ± 31.4	131.3 ± 31.0	0.8310
TC (mg/dl)	186.7 ± 35.7	185.1 ± 35.3	>0.9999
HDL (mg/dl)	56.4 ± 13.8	53.9 ± 13.2	0.6043
LDL (mg/dl)	114.1 ± 24.1	70.0 ± 10.0	0.0833
TC: HDL	3.5 ± 0.8	3.6 ± 0.9	0.7902
TG (mg/dl)	105.3 ± 49.9	231.4 ± 109.0	*0.0379
Glucose (mg/dl)	89.1 ± 6.8	85.3 ± 21.3	0.3427
Apolipoprotein B-100 (mg/dl)	80.4 ± 16.8	83.9 ± 15.7	0.6480

3.3 COX-2 induction elicits an athero-protective phenotype in HAEC

To determine the effect of COX-2 expression on endothelial inflammation, VCAM-1was measured by flow cytometry in HAEC exposed to varying TNFα doses with and without pharmacological intervention to manipulate COX. The following data originated with the doctoral dissertation of Dr. Anita Rajamani and has been updated and revised to include additional donors. Dr. Rajamani conducted extensive dose response experiments to determine the IC_{50} for the inducers and inhibitors in HAEC.[42] VCAM-1 expression was stimulated by TNFα in a dose-dependent manner. This expression was completely abrogated in HAEC stimulated with the COX-2 inducer PDBu. This aligns with COX-2 having an athero-protective role; despite increased cytokine stimulation, VCAM-1 is not upregulated in the presence of COX-2 induction (figure 3.3.1-A). In contrast, HAEC stimulated with the COX-2 inhibitor rofecoxib displayed no

significant differences in VCAM-1 expression from the TNFα dose controls (figure 3.3.1-B). Likewise, HAEC stimulated with indomethacin, an inhibitor of both COX-1 and -2, displayed no significant differences from the TNFα dose controls (figure 3.3.1-C).

To examine a role for endothelial metabolism by COX-2 in mediating an inflammatory response to subjects' TGRL, HAEC VCAM-1 surface expression was measured while manipulating COXs through pharmacological intervention. HAEC were exposed to TNFα (EC_{50} for CAMs upregulation) and pro-inflammatory TGRL, in the presence and absence of inducers or inhibitors of COX. VCAM-1 surface expression was analyzed via flow cytometry and presented as % change from the TNFα control. HAEC stimulated in the presence of PDBu demonstrated a significant downregulation of TGRL-induced VCAM-1 surface expression (figure 3.3.1-D), completely shifting the VCAM-1 response to promote an anti-inflammatory phenotype. Unexpectedly, HAEC stimulated in the presence of the COX-2-specific inhibitor rofecoxib also demonstrated a significant downregulation of TGRL induced VCAM-1 surface expression, although not to the same degree as PDBu (figure 3.3.1-E). There was a significant difference between the two treatments in VCAM-1 % change expression when compared to their respective TGRL control points (figure 3.3.2). However, HAEC stimulated with indomethacin that inhibits both COX-1 and COX-2 demonstrated no significant effect on TGRL-induced VCAM-1 surface expression compared to the control (figure 3.3.1-F). Together these data reveal a powerful effect of COX-2 on endothelial inflammation that aligns with its known athero-protective role, and further implicate a direct role in the metabolism of TGRL by endothelium. Furthermore, western blot data revealed COX-1 was constitutively expressed in HAEC (figure 3.3.3). The data suggest that COX-1 may take on an athero-protective role when COX-2 is

inhibited, and/ or that cross talk with other metabolic pathways is also playing a role to prevent VCAM-1 expression from increasing.

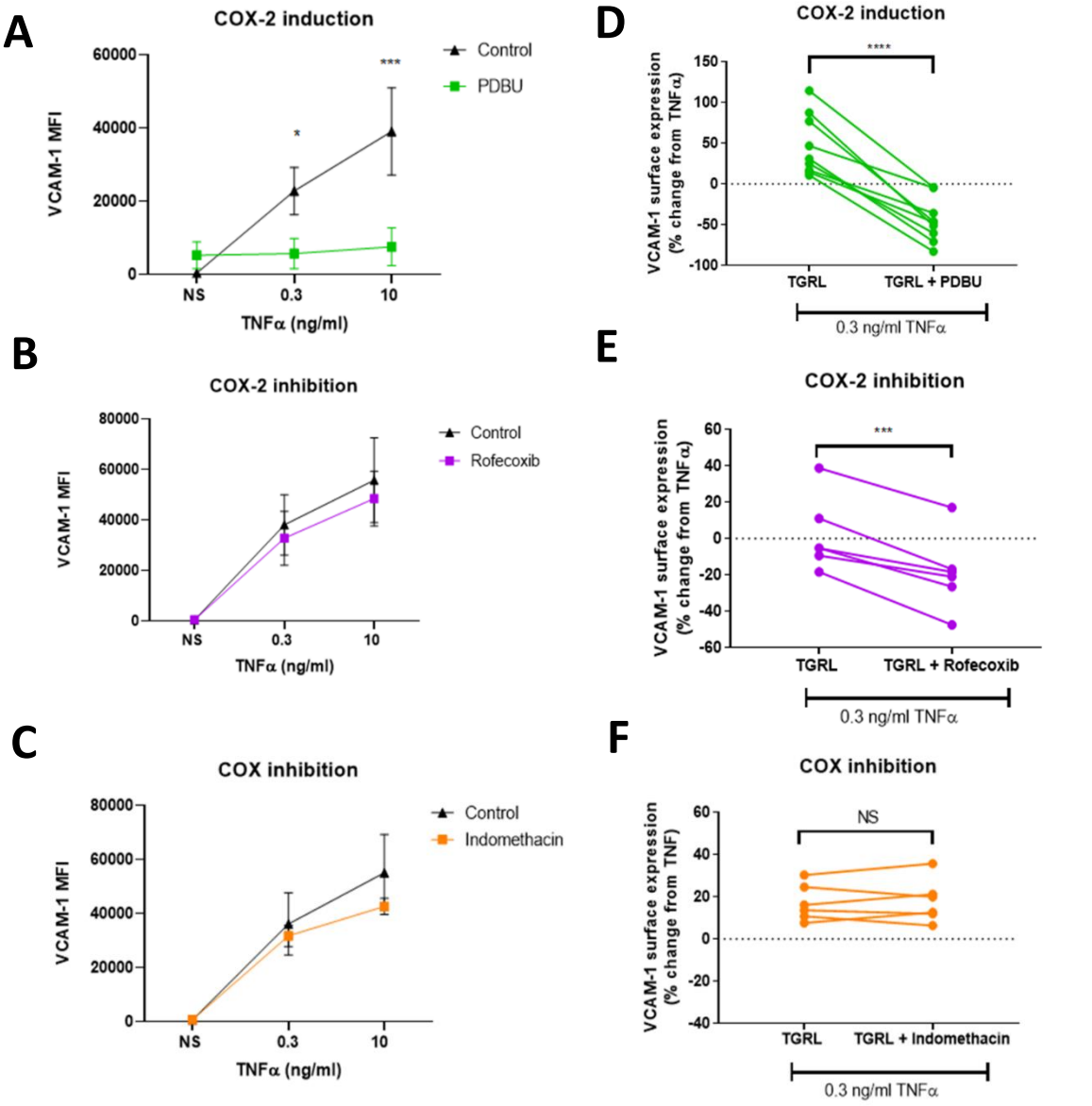

*Figure 3.3.1: (A) HAEC were pretreated with PDBu (1 µM, 1h) followed by combined treatment of PDBu and TNFα doses for 4 hours. VCAM-1 MFI by flow cytometry analysis is seen in A. (B) HAEC were pretreated with PDBu (1 µM, 1h) followed by combined stimulation of pro-atherogenic TGRL and TNFα (EC_{50} CAM upregulation) for 4 hours with and without PDBu treatment. VCAM-1 surface expression as a % change from the control without TGRL is seen in B. (C) HAEC were pretreated with rofecoxib (1 µM, 1h) followed by combined treatment of rofecoxib and TNFα doses for 4 hours. VCAM-1 MFI from flow cytometry analysis is seen in C. (D) HAEC were pretreated with rofecoxib (1 µM, 1h) followed by combined stimulation of pro-atherogenic TGRL and TNFα (EC_{50} CAM upregulation) for 4 hours with and without rofecoxib treatment. VCAM-1 surface expression as a % change from the control without TGRL is seen in D. (E) HAEC were pretreated with indomethacin (1 µM, 1h) followed by combined treatment of indomethacin and TNFα doses for 4 hours. VCAM-1 MFI from flow cytometry analysis is seen in E. (F) HAEC were pretreated with indomethacin (1uM, 1hr) followed by combined stimulation of pro-atherogenic TGRL and TNFα (EC_{50} CAM upregulation) for 4 hours with and without indomethacin treatment. VCAM-1 surface expression as a % change from the control without TGRL is seen in F. Values are means ± SD. *p <0.05, ***p < 0.0005 for A, C, E represents significant changes in VCAM-1 with and without pharmacological intervention. ***p <0.0005, p < 0.0001 for B, D, E represents significant changes in VCAM-1 surface expression when compared to the TGRL control. n=6-9*

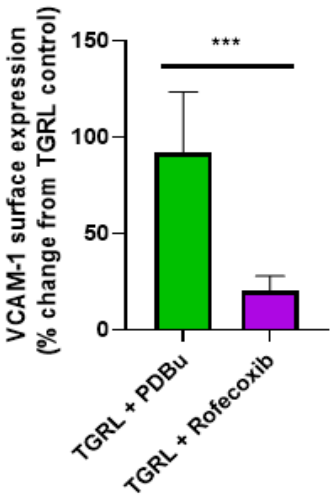

*Figure 3.3.2: VCAM-1 % change in the presence of PDBu and rofecoxib when compared to their respective TGRL VCAM-1 controls. Data is from figure 3.3.1-D, E datasets. TGRL + PDBu vs TGRL + Rofecoxib ***p < 0.0005, unpaired t-test. n = 6-9.*

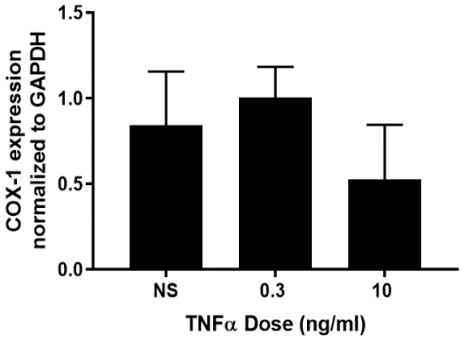

Figure 3.3.3: HAEC were stimulated with varying doses of TNFα (NS, 0.3-EC_{50} for CAM upregulation, and 10 ng/ml) for 4 hours, were lysed and used for western blot. COX-1 expression is normalized to GAPDH. n = 3.

3.4 COX-2 expression is ER stress-dependent

To further elucidate a potential effect of COX-2 expression on the ER stress mechanism driving endothelial inflammation, Western blot experiments were conducted while manipulating COX-2 expression using pharmacological interventions and COX-2 siRNA knockdown. HAEC were pre-treated with PDBu (1 µM), rofecoxib (1 µM), or DMSO for 1 h and incubated for 4 h at 37 ºC with TNFα (EC_{50} of CAM upregulation) and a treatment as described above. To confirm the results using the COX-2 inhibitor rofecoxib, COX-2 siRNA was used as an alternative method to suppress its expression. Figure 3.4.1 displays COX-2 protein expression normalized to GAPDH loading control using both rofecoxib and COX-2 siRNA as methods of COX-2 inhibition. COX-2 siRNA transfection was successful in achieving a significant 87% knockdown, to a level comparable to that achieved with rofecoxib. In contrast, PDBu significantly increased COX-2 expression compared to the scrambled control. These data confirmed that a 4 h incubation was sufficient to elicit a significant effect on COX-2 protein

levels. Moreover, the general ER stress inhibitor 4-PBA reduced COX-2 expression (figure 3.4.2), although not to a significant extent, implying that COX-2 expression may be ER stress dependent. Therefore, we then further explored the ER stress response pathways to determine whether COX-2 modulation can regulate ER stress-mediated VCAM-1 expression in HAEC.

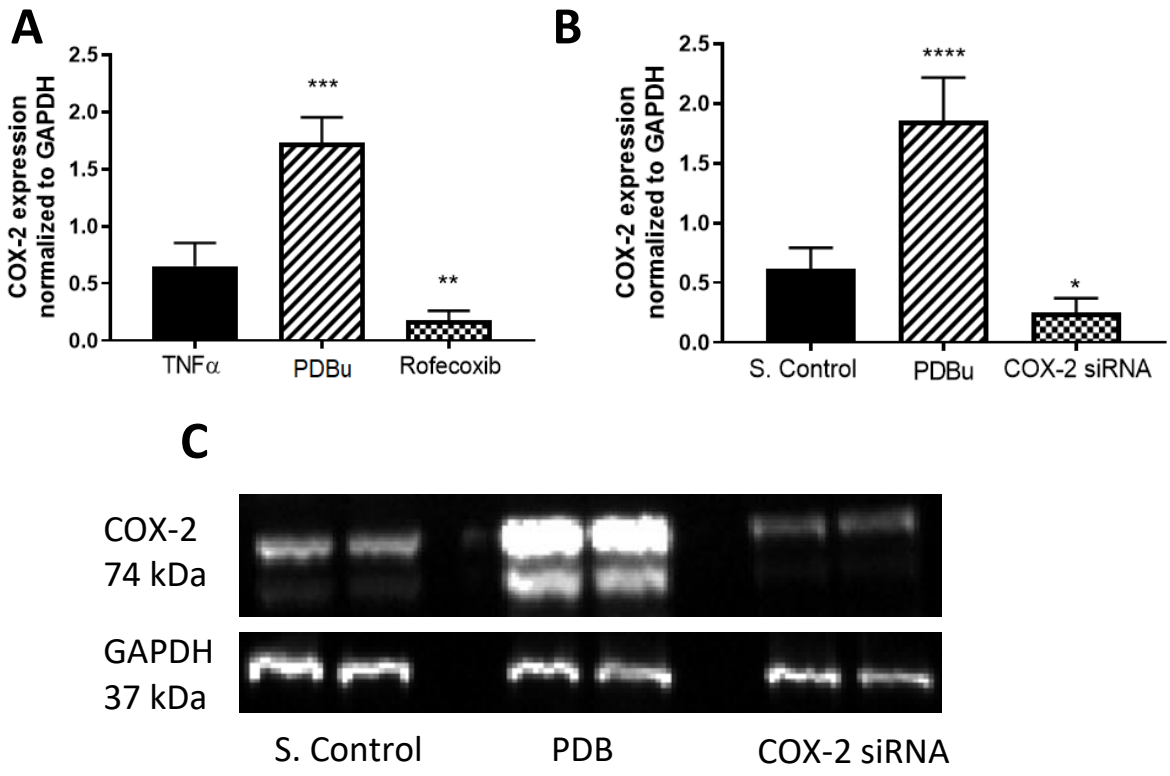

*Figure 3.4.1: HAEC stimulated with TNFα (EC_{50} for CAM upregulation) and incubated with scrambled control, PDBu, rofecoxib, or COX-2 siRNA for 4 h were lysed and used for western blot. (A) COX-2 expression normalized to GAPDH is measured from cell lysates with rofecoxib as the source for COX-2 inhibition. (B) COX-2 expression normalized to GAPDH is measured from cell lysates with COX-2 siRNA as the source for COX-2 inhibition. (C) Representative images from western blot measuring COX-2 and GAPDH expression when stimulated with TNFα (EC_{50} of CAM upregulation) and scrambled control, PDBu, or COX-2 siRNA. Values are means ± SD. *p <0.05, **p <0.001, ***p <0.0005, **** p <0.0001 represents significant changes in expression when compared to the control (DMSO or scrambled). n =5.*

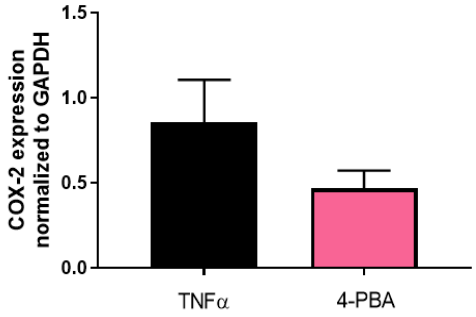

*Figure 3.4.2: HAEC stimulated with TNFα (EC_{50} for CAM upregulation) and incubated with the ER stress inhibitor, 4-PBA, for 4 h were lysed and used for western blot. COX-2 expression normalized to GAPDH is measured from cell lysates. Values are means ± SD. *p < 0.05 between control vs 4-PBA. n = 3.*

3.5 COX-2 manipulation regulates the ER stress response

To further determine the connection between COX-2 and the ER stress response pathways, several ER stress markers were analyzed while manipulating COX-2 expression. HAEC were pre-treated with DMSO (control), PDBu, or rofecoxib (1 µM, 1 h) and then incubated with TNFα (EC_{50} CAM upregulation) and the treatment (1 µM) for 4 h at 37 ºC. Cells were then lysed and used to explore ER stress markers via Western blot (figure 3.5.1). The endoplasmic reticulum chaperone BiP is an upstream regulator of the UPR that was seen to decrease significantly when COX-2 was inhibited by rofecoxib. COX-2 induction by PDBu also decreased BiP expression (figure 3.5.1-A). Consistent with the results for BiP, sXBP-1 was significantly decreased by both induction and inhibition of COX-2 (figure 3.5.1-B). IRF-1, the transcription factor that promotes maximal VCAM-1 expression downstream of sXBP-1 activation, was significantly decreased when COX-2 was inhibited (figure 3.5.1-C). In contrast, the ratio of phosphorylated iRE1α to total iRE1α was increased by COX-2 induction or inhibition, though not significantly (figure 3.5.1-D). These data though confounding support a

link between COX-2 expression and ER stress. These results may imply crosstalk with other metabolic pathways, such as CYP/sEH.

To validate the results observed when using rofecoxib as the source of COX-2 inhibition, ER stress markers were also examined using siRNA-mediated knockdown of COX-2. HAEC were pre-treated with DMSO or PDBu (1 μM, 1 h) and then incubated with TNFα (EC_{50} CAM upregulation) and scrambled control, PDBu, or COX-2 siRNA for 4 h at 37 ºC. Cells were then lysed and used to explore ER stress markers via western blot (figure 3.5.2). Consistent with the results when using rofecoxib, BiP was seen to decrease significantly when COX-2 was inhibited via COX-2 siRNA transfection, as was sXBP-1 (figure 3.5.2-A, B). IRF-1 was decreased when COX-2 was either induced or inhibited, though not significantly (figure 3.5.2-C). The ratio of phosphorylated iRE1α to total iRE1α was significantly increased when COX-2 was induced and by COX-2 knockdown (figure 3.5.2-D). P-eIF2α, a marker associated with another arm of the ER stress response, was significantly upregulated by PDBu, but not by COX-2 silencing (figure 3.5.2-E). Overall, COX-2 siRNA transfection produced similar results to pharmacological inhibition of COX-2 for BiP, IRF-1, sXBP-1, and the iRE1α ratio. These results may further support the idea of crosstalk with other metabolic pathways as a mechanism for regulation of COX-2 mediated ER stress. However, in the absence of other stimuli these data do not strongly support a role for COX-2 in modulating ER-stress mediated regulation of TNFα-induced VCAM-1 expression, but rather changes in cellular responses that inversely influence the expression of these two proteins.

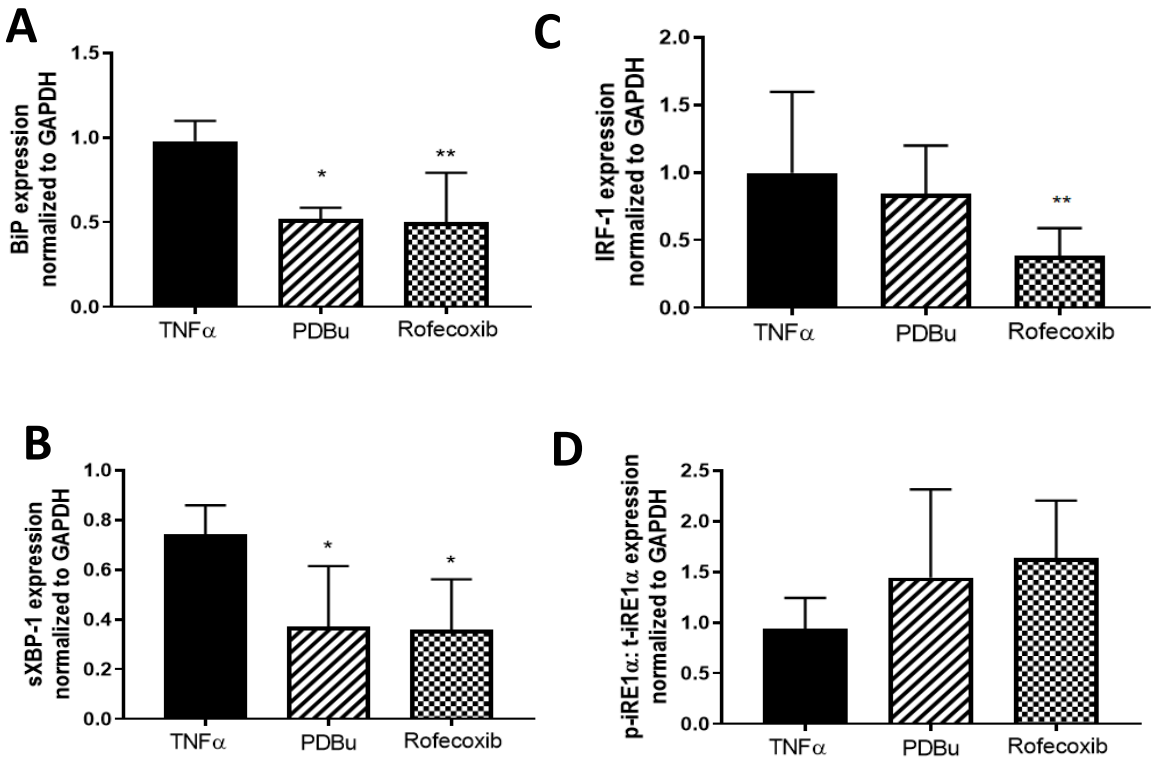

*Figure 3.5.1: HAEC stimulated and incubated with TNFα (EC_{50} for CAM upregulation) and DMSO, PDBu, or rofecoxib for 4 hours were lysed and used for western blot. (A) BiP expression normalized to GAPDH, (B) IRF-1 expression normalized to GAPDH, (C) sXBP-1 expression normalized to GAPDH, (D) p-iRE1α: t-iRE1α expression normalized to GAPDH is measured from cell lysates. Values are means ± SD. *p < 0.05, **p < 0.001 represents significant changes in expression when compared to the control (TNFα-DMSO). n = 3-5.*

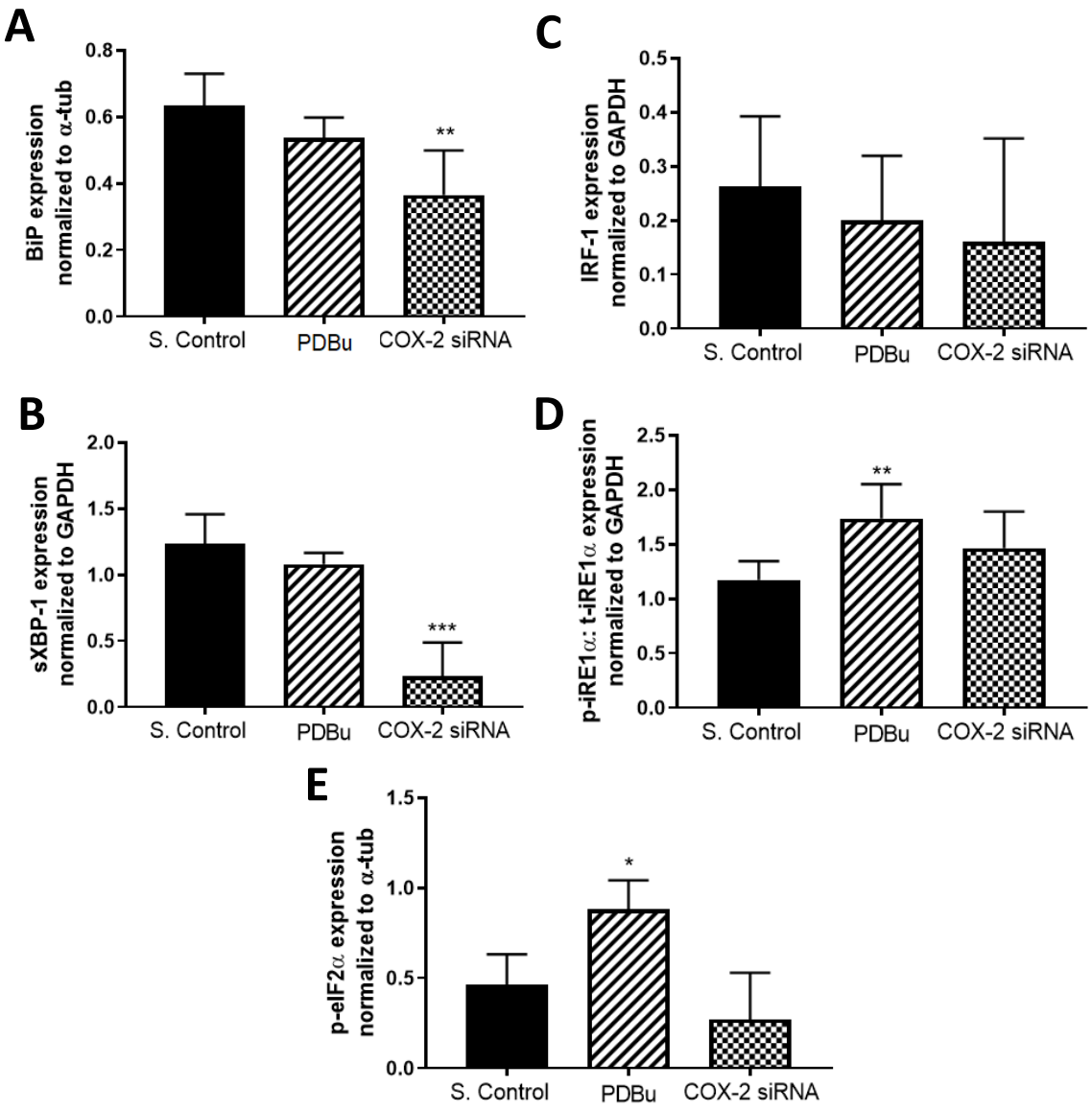

*Figure 3.5.2: HAEC stimulated and incubated with TNFα (EC_{50} for CAM upregulation) and scrambled control, PDBu, or COX-2 siRNA for 4 hours were lysed and used for western blot. (A) BiP expression normalized to GAPDH, (B) IRF-1 expression normalized to GAPDH, (C) sXBP-1 expression normalized to GAPDH, (D) p-iRE1α: t-iRE1α expression normalized to GAPDH, (E) p-eIF2α normalized to α-tub is measured from cell lysates. Values are means ± SD. *p < 0.05, **p < 0.001, ***p < 0.0005 represents significant changes in expression when compared to the scrambled control). n = 3-5.*

3.6 Pro-inflammatory TGRL elicits variable ER stress response under static conditions

In contrast to TNFα-induced VCAM-1, which is partially dependent on an ER stress response, we previously showed that inhibiting ER stress completely abrogated the increase in VCAM-1 expression elicited by pro-inflammatory TGRL. Having demonstrated that COX-2 manipulation alters the expression of ER stress markers, we next investigated a role for COX-2 in mediating the ER stress response leading to enhanced VCAM-1 expression by pro-inflammatory TGRL in HAEC. Pro-inflammatory TGRL were characterized via flow cytometry and on average increased VCAM-1 expression 30% relative to TNFα alone. HAEC were pre-treated with DMSO (control), PDBu, or rofecoxib (1 uM, 1 hour) and then incubated with TNFα (EC_{50} CAM upregulation), the treatment (1 uM), and pro-inflammatory TGRL (10 mg/dl ApoB) for 4 hours at 37 C. Cells were then lysed and used to explore ER stress markers via western blot (figure 3.6.1).

TNFα controls with COX-2 manipulation were compared to the groups stimulated with TNFα, COX-2 pharmacological intervention, and pro-inflammatory TGRL. Significant changes between intervention groups were denoted by asterisk for all ER stress markers and COX-2 expression. BiP was seen to decrease significantly with the addition of pro-inflammatory TGRL. IRF-1 was significantly decreased in the presence of pro-inflammatory TGRL for both the control and COX-2 induction conditions. sXBP-1 was significantly upregulated by pro-inflammatory TGRL in the PDBu condition. The ratio of phosphorylated iRE1α to total iRE1α had no significant effect in the presence of pro-inflammatory TGRL. Lastly, pro-inflammatory TGRL significantly increased COX-2 expression in the PDBu condition. COX-2 induction with pro-inflammatory TGRL significantly increased sXBP-1 and COX-2 but didn't appear to have significant effects on the other ER stress markers, suggesting perhaps other mechanisms are

involved in the regulation of inflammation since TGRL is known to elicit VCAM-1 upregulation compared to baseline. COX-2 inhibition with pro-inflammatory TGRL had no significant effects on the ER stress markers or COX-2, further suggesting other mechanisms are involved in ultimately regulating VCAM-1 when induced with TGRL. These results also suggest that COX-2

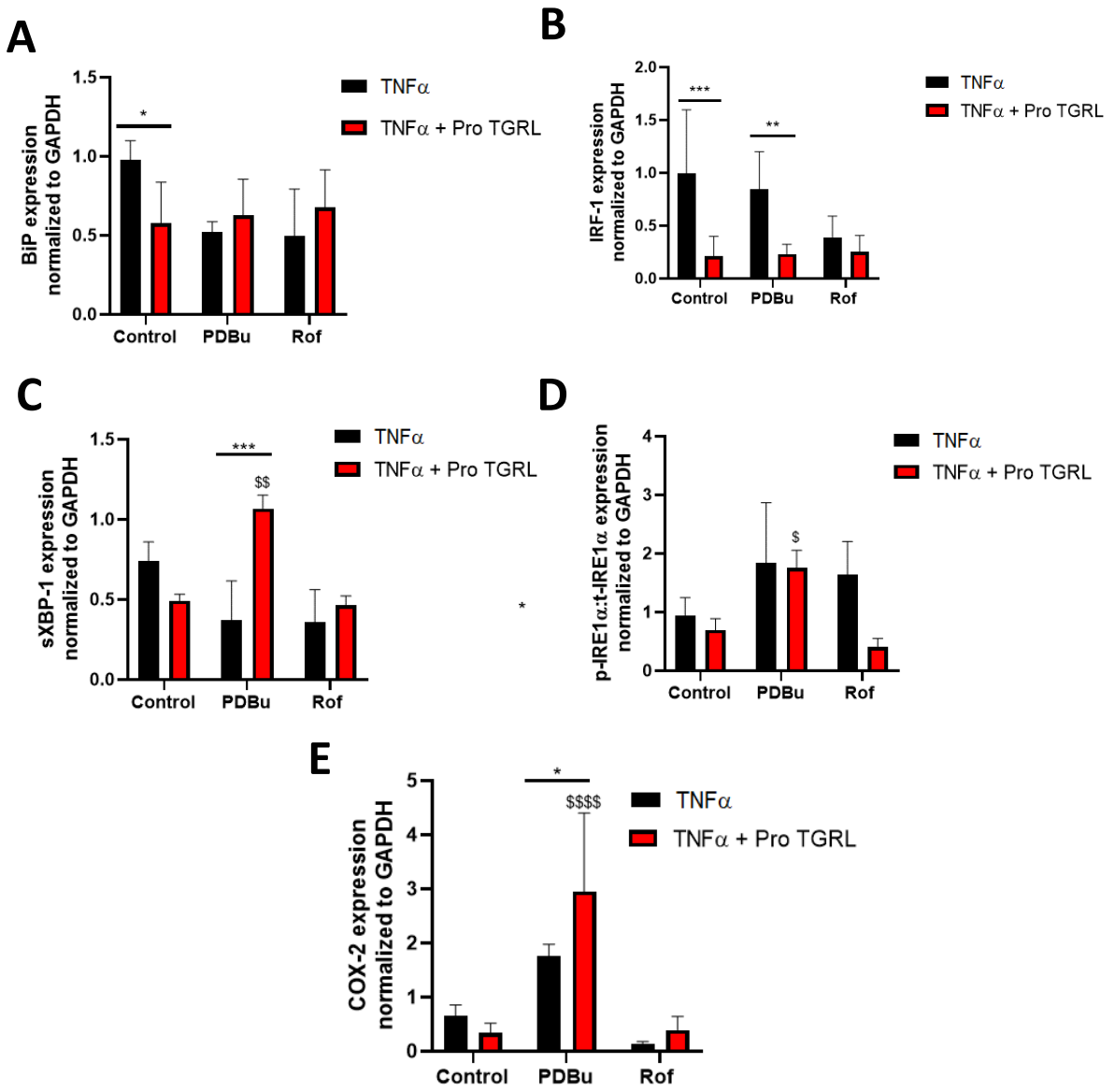

*Figure 3.6.1: HAEC stimulated and incubated with TNFα (EC_{50} for CAM upregulation) and DMSO (control), PDBu, or rofecoxib for 4 h were lysed and used for western blot. (A) BiP expression normalized to GAPDH, (B) IRF-1 expression normalized to GAPDH, (C) sXBP-1 expression normalized to GAPDH, (D) p-iRE1α: t-iRE1α expression normalized to GAPDH, (E) COX-2 normalized to GAPDH is measured from cell lysates. Values are means ± SD. *p < 0.05, **p < 0.001, ***p < 0.0005, **** p < 0.0001 between TNFα with and without the addition of pro-inflammatory TGRL. $ p < 0.05, $$ p < 0.001, $$$$ p < 0.0001 represents significant changes in expression when compared to the control. n = 3-5.*

manipulation is not directly connected to ER stress-mediated VCAM-1 regulation.

Moreover, figure 3.6.1 also demonstrates the significant changes of pro-inflammatory TGRL combined with pharmacological intervention compared to the control with just pro-inflammatory TGRL and no COX-2 manipulation. These changes are denoted by "$". COX-2, sXBP-1, and the ratio of phosphorylated iRE1α to total iRE1α were significantly increased in the presence of both PDBu and pro-inflammatory TGRL when compared to the TGRL control. Overall, the data suggests that the link between the COX-2 pathway and TGRL induced VCAM-1 expression is not acting directly through the ER stress mechanism alone.

3.7 Pro-inflammatory TGRL enhances COX-2 and VCAM-1 expression in inflamed HAEC

We previously demonstrated that low magnitude SS was a potent inducer of an ER stress response and was synergistic with pro-inflammatory TGRL in eliciting maximal VCAM-1 expression, as demonstrated in fig 3.7.1-A. The TNFα control data for both VCAM-1 and COX-2 is the same shown in figure 3.1.1. Since SS also promoted the upregulation of COX-2 which was shown to alter the inflammatory response to TGRL (fig 3.7.1-B), we next examined whether the SS modulation of COX-2 expression could be mechanistically linked to that of VCAM-1 expression in the Hele-Shaw AOC. The addition of pro-inflammatory TGRL to HAEC stimulated with TNFα for 4 h in the AOC significantly increased COX-2 expression over the entire SS range from 2-12 dynes/cm^2 compared to the TNFα static control as seen in figure 3.7.1 The results suggest that shear stress is synergistic with pro-inflammatory TGRL in stimulating robust COX-2 upregulation in inflamed HAEC. While VCAM-1 expression still peaked at 2 dynes/cm^2, pro-inflammatory TGRL had the effect of overall enhancing VCAM-1 expression significantly across 2-12 dynes/cm^2 relative to TNFα alone at the corresponding SS. Although

COX-2 is significantly upregulated at every shear stress magnitude when compared to the static control, the trend to further increase with shear stress is still observed. Notably, figure 3.7.1 also depicts VCAM-1 and COX-2 expression in the absence and presence of pro-inflammatory TGRL within the same endothelial monolayers, revealing different patterns of expression, where COX-2 expression is more sensitive to upregulation by pro-inflammatory TGRL across the entire shear stress gradient. The results are consistent with western blot data under static conditions.

Figure 3.7.2 demonstrates a simple linear regression analysis with a R^2 value of 0.8593, slope of -0.4906, and a p-value of 0.0078 for the pro-inflammatory TGRL, with the TNFα

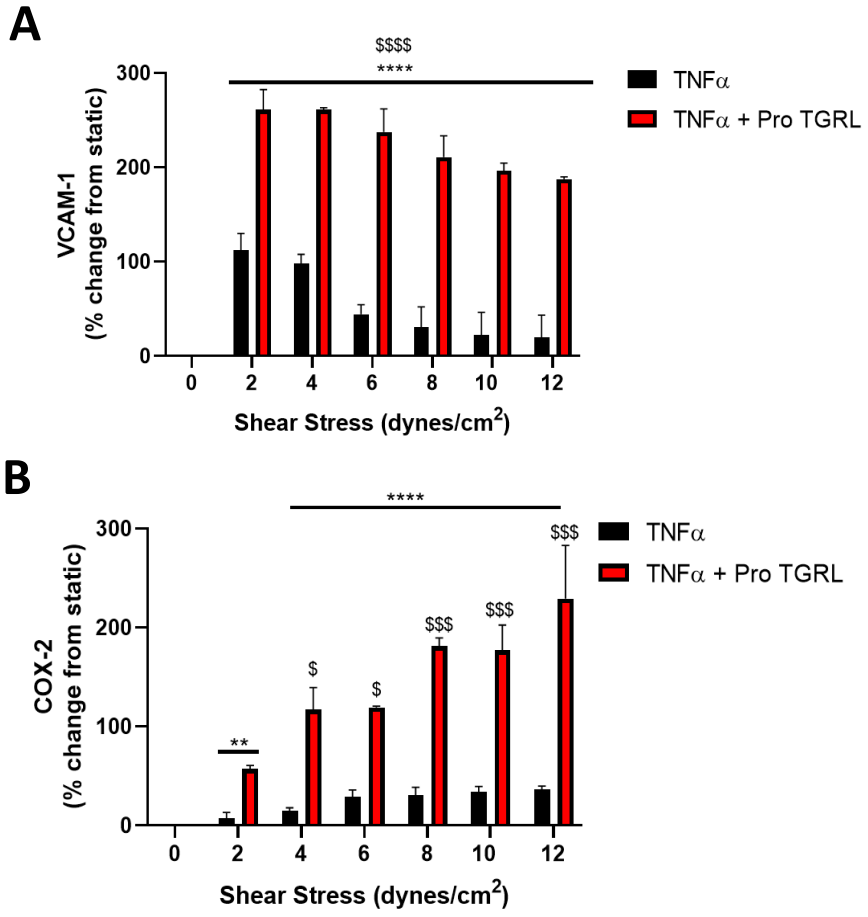

*Figure 3.7.1: VCAM-1 (A) and COX-2 (B) expression after a 4 h AOC flow run in the presence and absence of pro-inflammatory TGRL (10 mg/dl ApoB) across a shear stress gradient of 0-12 dynes/cm². HAEC were also stimulated with TNFα (EC_{50} for CAM upregulation). HAEC were imaged by confocal microscopy. Values are means ± SD. ****p < 0.0001 between Pro TGRL vs no Pro TGRL. $ p < 0.05, $$ p < 0.001, $$$ p < 0.0005, $$$$ p < 0.0001 represents significant changes in expression when compared to the static control. n = 3 slides.*

control present for comparison. An analysis of covariance was conducted to compare the two linear regressions and resulted in a p-value of 0.000013 indicating a significant statistical difference. The presence of pro-inflammatory TGRL in HAEC significantly upregulated VCAM-1 and COX-2 expression across the entire SS gradient. It also widened the COX-2 expression level range while narrowing VCAM-1 expression, significantly decreasing the slope magnitude. Additionally, the linear inverse relationship is still maintained in the presence of pro-inflammatory TGRL. This further demonstrates the significant inverse correlation between COX-2 and VCAM-1 in HAEC across the shear stress gradient when stimulated with TNFα and pro-inflammatory TGRL, consistent with the results seen with TNFα stimulation alone (figure 3.3.2).

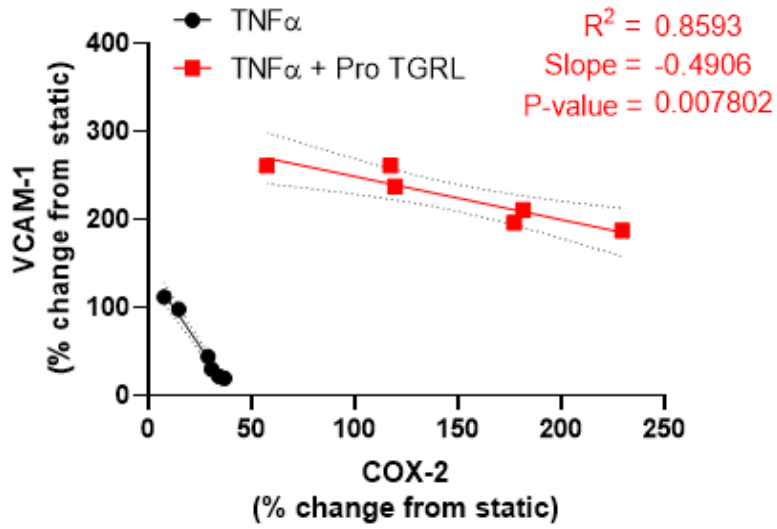

*Figure 3.7.2: Simple linear regression analysis showing the inverse correlation between COX-2 and VCAM-1 in HAEC stimulated with TNFα and pro-inflammatory TGRL (red) and the TNFα control (black) from figure 3.1.2. VCAM-1and COX-2 expression after a 4 h AOC flow run in the presence of TNFα (EC_{50} for CAM upregulation) and pro-inflammatory TGRL across a shear stress gradient of 0-12 dynes/cm^2. HAEC were imaged by confocal microscopy. Values are means ± SD. *p <0.05 correlation. n =3 slides.*

3.8 COX-2 induction and inhibition attenuates shear-induced VCAM-1 expression

To determine a possible role for COX-2 in the suppression of VCAM-1 expression elicited by cytokine at low magnitude SS, HAEC were exposed to TNFα and SS in the Hele-Shaw AOC for 4 h along with an inducer of COX-2, PDBu (1 μM). In general, the presence of PDBu attenuated VCAM-1 expression across the shear stress gradient (2-12 dynes/cm^2) compared to the TNFα control (figure 3.8.1). VCAM-1 was suppressed most dramatically and significantly at low magnitude shear stress (2-4 dynes/cm^2) where its expression was maximal in the absence of PDBu. In contrast, PDBu significantly upregulated COX-2 expression at 12 dynes/cm^2 compared to the TNFα control at the same shear stress magnitude. The 50% reduction in peak VCAM-1 expression under low shear was associated with a small but insignificant increase in COX-2 expression at this level, implicating the possible involvement of alternative mechanisms that indirectly link COX-2 with VCAM-1 expression. Enhanced COX-2 expression at high shear stress magnitudes, coinciding with low VCAM-1 expression, is consistent with an athero-protective role. Moreover, low magnitude SS appears to maintain a potent suppressive effect on COX-2 expression, even in the presence of the inducer.

To further assess the role of COX-2 in the regulation of endothelial VCAM-1 expression, AOC flow experiments were also conducted in the presence of rofecoxib, a COX-2 specific inhibitor. The addition of rofecoxib (1 μM) to the HAEC monolayer during a 4 h AOC flow run significantly suppressed VCAM-1 expression at 2-4 dynes/cm2, in a manner analogous to that induced by PDBu. COX-2 expression was significantly downregulated by rofecoxib at high shear stress magnitudes (8-12 dynes/cm2) as seen in figure 3.8.1. These results are consistent with rofecoxib's ability to block COX-2 expression elicited by high shear stress. An unexpected result was that the presence of rofecoxib decreased VCAM-1 expression across the shear stress

gradient (2-12 dynes/cm¬2). Exposure to this COX-2 inhibitor elicits roughly a 50% downregulation in VCAM-1 at low shear stress, similar to the COX-2 induction effect, suggesting that COX-2 manipulation is not directly linked to VCAM-1 regulation and other pathways are involved in the regulation.

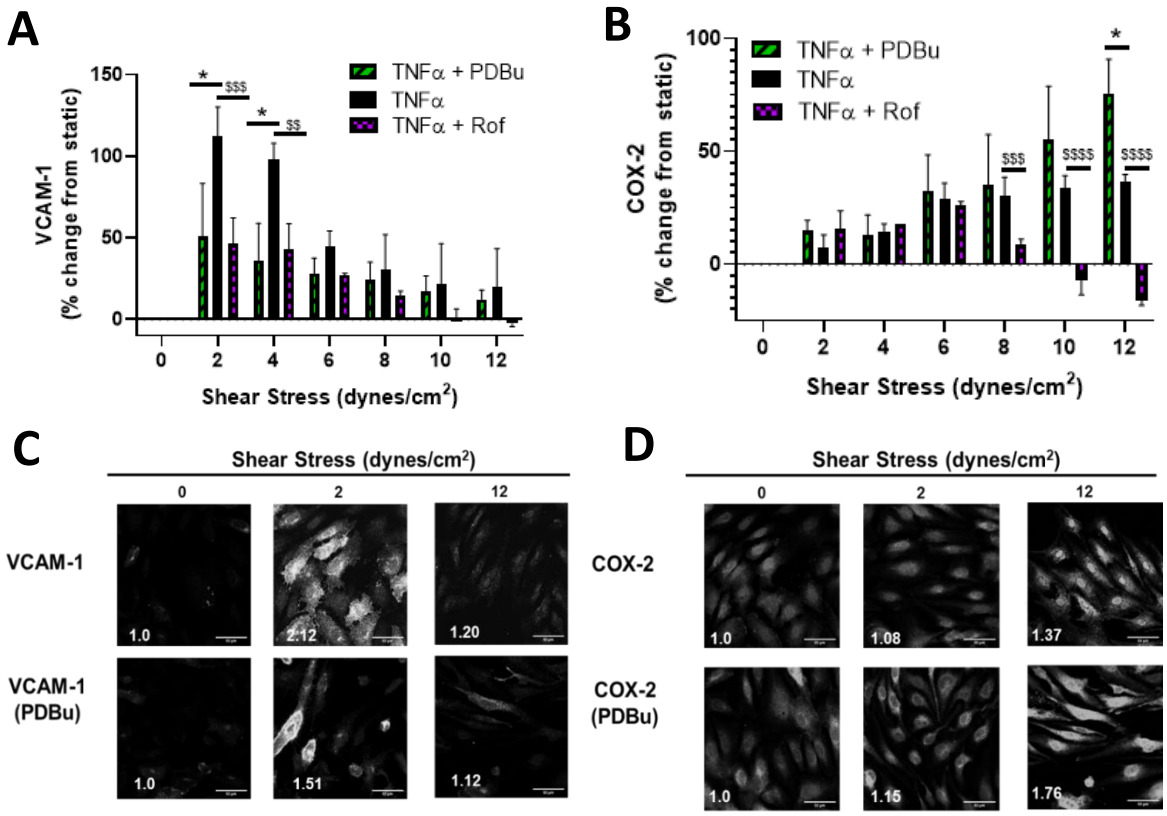

*Figure 3.8.1: VCAM-1 (A) and COX-2 (B) expression after a 4 h AOC flow run in the presence and absence of COX-2 inducer, PDBu (1 µM) and COX-2 inhibitor rofecoxib (1 µM) across a shear stress gradient of 0-12 dynes/cm² after a 1 h pre-treatment (1 µM). Representative images of VCAM-1 (C) and COX-2 (D) expression used for bar graph quantification (A, B) at 0, 2, and 12 dynes/cm². Scale bar = 50 µm. HAEC were imaged by confocal microscopy. Values are means ± SD. *p < 0.05 between PDBu vs no PDBu. $ p < 0.05, $$ p < 0.001, $$$ p < 0.0005, $$$$ p < 0.0001 rof vs no rof. n = 3-4 slides.*

3.9 COX-2 induction attenuates a shear stress-mediated ER stress response

To further assess the ramifications of COX-2 induction on a mechanism affecting VCAM-1 expression, we quantified the transcription factors sXBP-1 and IRF-1 associated with

an ER stress response previously shown promote maximum VCAM-1 expression by low SS. Nuclear expression of sXBP-1 and IRF-1 were analyzed after 2 h of stimulation and flow in the AOC. The addition of COX-2 inducer, PDBu (1 µM), to the HAEC monolayer significantly decreased sXBP-1 expression from 4-12 dynes/cm^2 compared to the TNFα control. PDBu did not have any significant effect on IRF-1 expression across the shear stress gradient when compared to the TNFα control, although a decreasing trend was observed at higher shear stress magnitudes. Downregulation of sXBP-1 and IRF-1 at high shear stress is consistent with previous observations. COX-2 induction at high shear stress suppresses ER stress mediated inflammation, consistent with a suppressive effect on VCAM-1 expression.

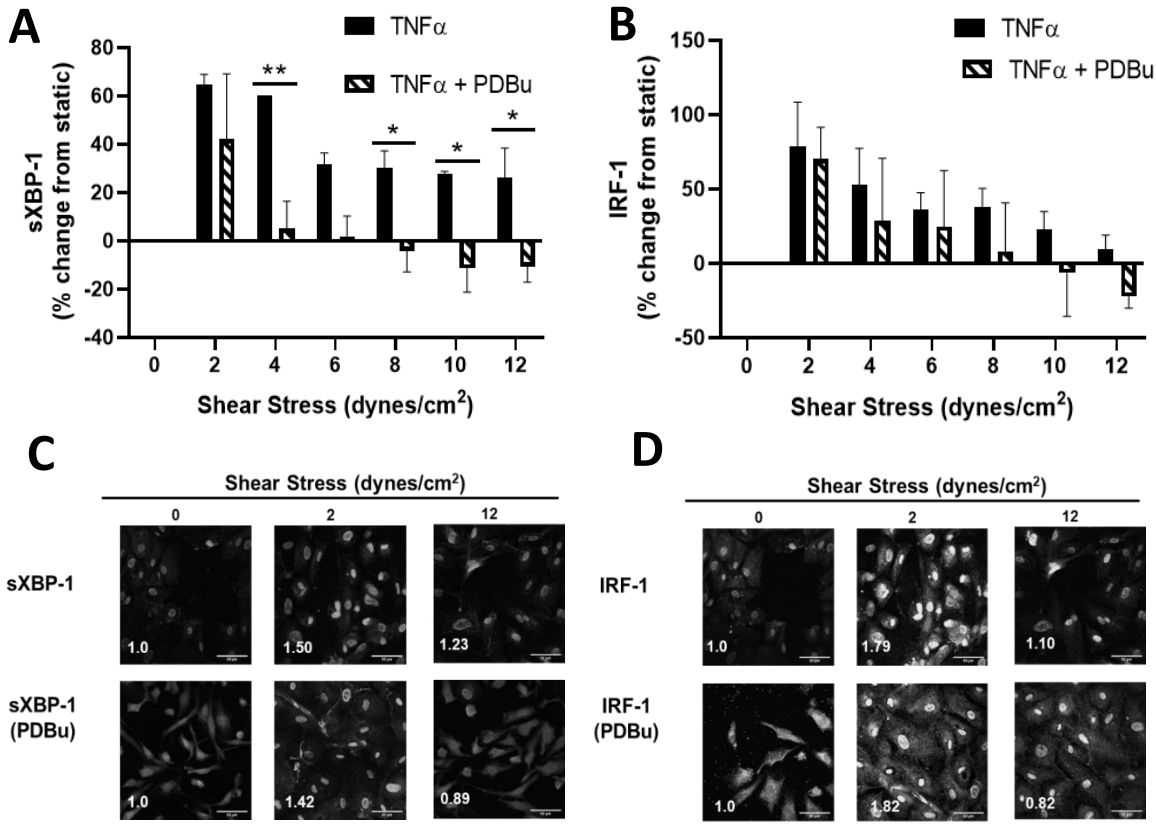

*Figure 3.9.1: sXBP-1(A) and IRF-1(B) expression after a 2 h AOC flow run in the presence and absence of COX-2 inducer, PDBu (1 µM) across a shear stress gradient of 0-12 dynes/cm^2 after a 1 h pre-treatment (1 µM). Representative images of sXBP-1 (C) and IRF-1 (D) expression used for bar graph quantification (A, B) at 0, 2, and 12 dynes/cm^2. Scale bar = 50 µm.HAEC were imaged by confocal microscopy. Values are means ± SD. *p < 0.05, ** P < 0.001 between PDBu vs no PDBu. n = 3 slides.*

DISCUSSION

The goal of this study was to begin to elucidate how endothelial metabolism of PUFA transported in an individual's TGRL can affect an inflammatory response promoting atherosclerosis. The initial focus on COX-2 was motivated by the observation that its expression increases in proportion to the level of shear stress and in the presence of TGRL acting on inflamed HAEC. Further, induction of COX-2 elicited a phenotypic shift in TGRL-treated HAEC, from pro- to anti-inflammatory, reflected in the surface expression of VCAM-1 relative to TNFα. We hypothesized that shifting PUFA metabolism via COX-2 manipulation would alter the ER stress-mediated and IRF-1-induced VCAM-1 upregulation induced by pro-inflammatory TGRL. Specifically, we expected COX-2 induction to suppress ER stress-mediated VCAM-1 expression, and COX-2 inhibition to promote such a response. These results are in general consistent with a documented protective role for COX-2 in reducing endothelial inflammation that promotes atherosclerosis and reveal the potential for endothelial PUFA metabolism to modulate an inflammatory response to TGRL. However, although there was a strong inverse correlation between the expression of COX-2 and VCAM-1, and COX-2 modulation attenuated shear-induced VCAM-1 expression in HAEC across the shear stress gradient, the evidence did not strongly support a direct effect on the ER stress response, and the underlying mechanisms remain unclear. Moreover, confounding results upon induction and inhibition of COX-2 implicate a possible role for COX-2 and perhaps crosstalk with other pathways in mediating the observed responses. The study confirmed the potent effect of low shear stress to enhance VCAM-1 expression, which correlated directly with suppression of COX-2 expression, consistent with an atherosusceptible phenotype.

VCAM-1 and COX-2 demonstrated a significant inverse correlation across the shear stress gradient in the same HAEC monolayers with an $R^2 > 0.9$. COX-2 was expressed at a low level in unstimulated HAEC but upregulated by TNFα, demonstrating the need for cytokine stimulation to elicit a variable response to SS. Its expression was further enhanced by high magnitude (atheroprotective) shear stress in the AOC device, registering a 37% increase from static control at 12 dynes/cm^2. COX-2 expression in the flow field negatively correlated with that of VCAM-1, which displayed a characteristic peak at a low (atherosusceptible) SS of 2 dynes/cm^2, consistent with previous reports.[2,4]

In this context we examined the effect of TGRL isolated from individual subjects to elicit a pro-inflammatory response that promotes atherosclerosis. TGRL characterized as pro-inflammatory via flow cytometry as increasing VCAM-1 expression by >10% from TNFα were used to investigate the role of COX-2 on inflammation. Elevated TG is a clinical risk factor for ASCVD, and there was a significant increase in TG postprandially in both pro- and anti-inflammatory donors as demonstrated in previous lab findings.[9] Pro-atherogenic TGRL also correlated with larger waist circumference and BMI as published in previous studies and confirmed here.[9,37]

COX-2 induction altered the pro-inflammatory response elicited by TGRL from human subjects, not only eliminating the average 50% increase in VCAM-1 expression relative to TNFα baseline, but further suppressing it by 50%. These changes in VCAM-1 expression are of pathological relevance since they were previously shown to correlate strongly with inflammatory monocyte adhesion.[2,4] Furthermore, the ability of COX-2 induction to dramatically alter the response to TGRL would implicate a role in metabolism of PUFA contained within these lipoproteins, as well as potentially other lipids and fatty acids.[52, 53] COX-2 induction shifting the

HAEC response from a pro-inflammatory phenotype to anti-inflammatory phenotype is consistent with reports of COX-2 playing an atheroprotective role. A study showed that homocysteine-induced monocyte adhesion in HAEC was decreased by COX inhibition using both indomethacin, non-selective COX-1/2 inhibitor and NS-398, a COX-2 selective inhibitor, which aligns with our observation of downregulation of VCAM-1 expression observed when COX-2 is exposed to rofecoxib in HAEC at atherosusceptible, low shear stress (figure 3.8.1).[44] Moreover, the effect of dual inhibition of COX-2 and COX on pro-inflammatory TGRL-induced VCAM-1 regulation might suggest that COX-1 takes on an atheroprotective role when necessary and other metabolic pathways are involved in crosstalk, but this can't be confirmed without an analysis of the metabolites produced by EC. Studies utilizing dual inhibition of COX-2 and sEH, have demonstrated crosstalk between the two pathways in inhibiting inflammation.[40] Moreover, researchers have shown that inhibition of COX-1/2 by NSAIDs shifts the arachidonic acid substrate towards other PUFA metabolic pathways, suggesting that dual inhibition of COX and sEH is necessary to elicit an anti-inflammatory response.[41] Thus, the sEH pathway may be involved in VCAM-1 regulation, which would explain some of the unexpected results using COX-2 manipulation. Specifically investigating the potential of such substrate shunting should be prioritized in future investigations.

In the presence of ER stress inhibitor (4-PBA) COX-2 was downregulated, demonstrating that COX-2 expression is influenced by ER stress. These results are consistent with COX-2 expression being downregulated by ER stress inhibitor 4-PBA, in vascular smooth muscle cells (VSMCs).[39] COX-2 manipulation affected ER stress downstream of its expression under static conditions, although this doesn't appear sufficient to explain the effects of COX-2 manipulation on VCAM-1 expression, as highlighted by the similar effects of COX-2 induction and inhibition

(figure 3.5.1). COX-2 siRNA transfection validated the results of COX-2 pharmacological inhibition lending credence to these results, and further supporting the hypothesis that crosstalk with other pathways, and mechanisms beyond ER stress are associated with the effects of COX-2 (figure 4.1). Other mechanisms may additionally be affecting VCAM-1 regulation, such as TNFα-induced p38 or other PUFA metabolic pathways (e.g., CYP/sEH, LOX) as reported in BAEC and HUVEC in previous studies.[5,10] Moreover, the addition of pro-inflammatory TGRL to these static experimental tests was shown to activate ER stress pathways and mediate an endothelial inflammatory response as reported by other findings (figure 3.6.1).[3] COX-2 induction with pro-inflammatory TGRL significantly increased sXBP-1 but also significantly decreased IRF-1 expression, consistent with a TGRL-induced VCAM-1 downregulation in the presence of PDBu under static conditions (figure 3.3.1). However, it is important to note that the IRF-1 response to pro-inflammatory TGRL was unexpected when comparing it to the effects of upstream ER stress markers like sXBP-1. Because IRF-1 is downstream sXBP-1, this means other mechanisms and/or pathways indirectly link COX-2 and VCAM-1 regulation, e.g., the NF-κB signaling pathways. Because sXBP-1 is significantly upregulated under the same conditions, other ER stress markers from different arms, such as PERK and p-eIF2α may additionally be affecting IRF-1 expression.

Overall, there is disparity between the current results and our previous work linking VCAM-1 upregulation to ER stress activation and IRF-1 expression in response to TGRL characterized as pro-inflammatory. Because the results of the ER stress markers were consistent when using COX-2 pharmacological inhibition and siRNA transfection, this suggests the unexpected results might be due to the involvement of other mechanisms or off-target effects of the methods of manipulating COX-2. Possible discrepancies might be due to inadequate

stimulation and atypical responses to TNFα in HAEC, using cells from different flasks for experiments with pro-inflammatory TGRL, and perhaps not mixing the pro-inflammatory TGRL stock well enough before aliquoting.

Previous studies have shown that pro-inflammatory TGRL can act to double VCAM-1 expression relative to the TNFα control across 2-12 dynes/cm^2.[2] Here VCAM-1 expression was significantly upregulated by pro-inflammatory TGRL across the shear stress gradient, consistent with published data.[2] In light of the documented protective effects of COX-2 on athero-inflammation, the significant COX-2 upregulation by TNFα and its enhancement in the presence of pro-inflammatory TGRL across the AOC shear stress gradient when compared to the TNFα control may reflect a feedback mechanism to check exuberant inflammation. Indeed COX-2 expression is downstream of TNFα-induced NF-κB. TGRL significantly enhanced VCAM-1 and COX-2 expression across the SS gradient, consistent with an enhanced TNFα response through NF-κB observed in previous studies.[38] In this study, SS had a potent modulatory effect on COX-2 expression under inflammatory stimulation. Atheroprotective high shear stress is correlated with an upregulation of KLF2, and studies have shown that elevated levels of KLF2 have enhanced COX-2.[35,36] Moreover, a study has shown that a dual COX/5-LOX inhibitor, ZLJ-6, attenuated TNFα-induced VCAM-1 and ICAM-1 expression in human umbilical vein endothelial cells (HUVECs) via a NF-κB pathway in both static and dynamic settings.[45] Because the study concluded that the effects on VCAM-1 were mediated by NF-κB as opposed to COX-2 or 5-LOX, this could be a possibility to explain the results in the current study as well.

Furthermore, previous studies have reported that ICAM-1 is enhanced at high shear stress regions.[5] Because ICAM-1 is independent of the ER stress mechanism and displays a similar pattern of expression, COX-2 expression could possibly be affected by a similar mechanism to

that driving ICAM-1 expression. For example, in addition to KLF2, the pattern of ICAM-1 expression may be more dependent upon transcription factors such as NF-κB and AP-1. Activation of p38 vs ERK1/2 MAP kinases were also shown to distinguish the mechanisms leading to VCAM-1 expression vs ICAM-1 expression, respectively, in the Hele-Shaw AOC shear gradient.[5] Studies have shown that PGE_2 induced ICAM-1 expression via a p38 MAPK/NF-κB signaling pathway in bEnd.3 brain endothelial cells.[46,47] Furthermore, effects of NSAIDs on HUVECs elucidated the involvement of NF-κB-independent pathways promoting ICAM-1 and COX-2.[48] Studies have demonstrated a relationship between COX-2 and ICAM-1 in fibroblasts, epithelial, and endothelial cells, and have suggested a mechanistic link via MAPK/NF-κB signaling pathways.[46-51] Thus, this could be an explanation as to why some of the ER stress markers results and VCAM-1 expression disparities are present.

In the Hele-Shaw AOC shear stress gradient, TNFα and TGRL-induced VCAM-1 and monocyte adhesion at low shear stress were significantly attenuated in the presence of ER stress inhibitor, 4-PBA, while ICAM-1 was unaffected.[4] Activation of an ER stress response culminating in enhanced IRF-1 activity was identified as a mechanism that distinguishes the maximal expression of VCAM-1 from that of ICAM-1. Because COX-2 expression was affected by ER stress inhibition, and pharmacological intervention does alter VCAM-1 response across the shear stress gradient, suppression of the ER stress pathways may contribute to the reduced inflammatory response, but other mechanisms such as those shared with ICAM-1 may also explain the effect of COX-2 manipulation on VCAM-1 expression.

COX-2 induction with PDBu attenuated VCAM-1 across the SS gradient, notably reducing peak expression by 62%. This suppression was in part attributable to inhibition of the ER stress response leading to VCAM-1 expression, as supported by ~50% reduction in ER stress

markers BiP and sXBP-1 (figure 3.5.1-A, B) and concomitant decrease in IRF-1 upon COX-2 induction (figure 3.5.1-C). PDBu attenuates TNFα induced VCAM-1, especially in atherosusceptible shear stress regions. Interestingly, COX-2 inhibition using rofecoxib within the AOC device also significantly attenuated VCAM-1 across 2-12 dynes/cm^2 by ~50% at atherosusceptible regions, to a similar extent as PDBu. Because COX-2 expression was significantly decreased at 8-12 dynes/cm^2 by more than 50% (figure 3.7.1), it confirms COX-2 inhibition is effective at atheroprotective regions. However, the results are consistent with those depicted in figure 3.5.1 where ER stress markers (e.g., BiP, IRF-1, sXBP-1) are downregulated in the presence of COX-2 inhibitor, rofecoxib. These results further support the idea that low shear stress effect has a potent effect to suppress COX-2 expression that overrides other stimuli. Moreover, since the effect of COX-2 induction to reduce CAM-1 expression at low shear stress did not correspond with a significant increase in COX-2 expression itself, an indirect link is implied.

COX-2 manipulation affects ER stress downstream of its expression under static conditions, although it isn't working alone to drive the regulation of VCAM-1 expression across a shear stress gradient. Other mechanisms may be affecting IRF-1-mediated VCAM-1 regulation. For example, TNFα-induced p38 enhanced ER stress-mediated VCAM-1 expression at low shear stress in previous studies.[5,10] Additionally, high shear stress elicited enhanced COX-2 expression in endothelial cells, which was found to be dependent on p38 through $\alpha_5\beta_1$ integrin-mediated signaling downstream of PECAM-1 mechanotransduction.[10] Moreover, because COX-2 doesn't increase significantly at low shear stress regions in the presence of PDBu as observed under static conditions (figure 3.4.1), this suggests low shear stress is very potent and overrides the mechanisms driving enhanced expression of COX-2. PDBu did not have any significant

effect on IRF-1 expression across the shear stress gradient when compared to the TNFα control, although a decreasing trend was observed at higher shear stress magnitudes which is consistent with static western blot results (figure 3.5.1) and VCAM-1 expression under the same conditions. In the absence of PDBu, sXBP-1 and IRF-1 expression is consistent with previous studies in which they were suppressed at atheroprotective regions.[4,5]

Figure 4.1 is a schematic illustrating how the results of the current study add to our understanding of the mechanisms driving pro-atherogenic VCAM-1 expression in HAEC. The results from various studies mentioned throughout the discussion were used to develop this potential signaling schematic. Solid black lines with arrows indicate knowns based on experimental conditions and results from this study and other previous studies, orange lines indicate COX pharmacological intervention, blue lines indicate the involved ER stress response investigated in this study, purple lines indicate potential crosstalk and pathways that may be involved in the COX-2 and VCAM-1 regulation link.

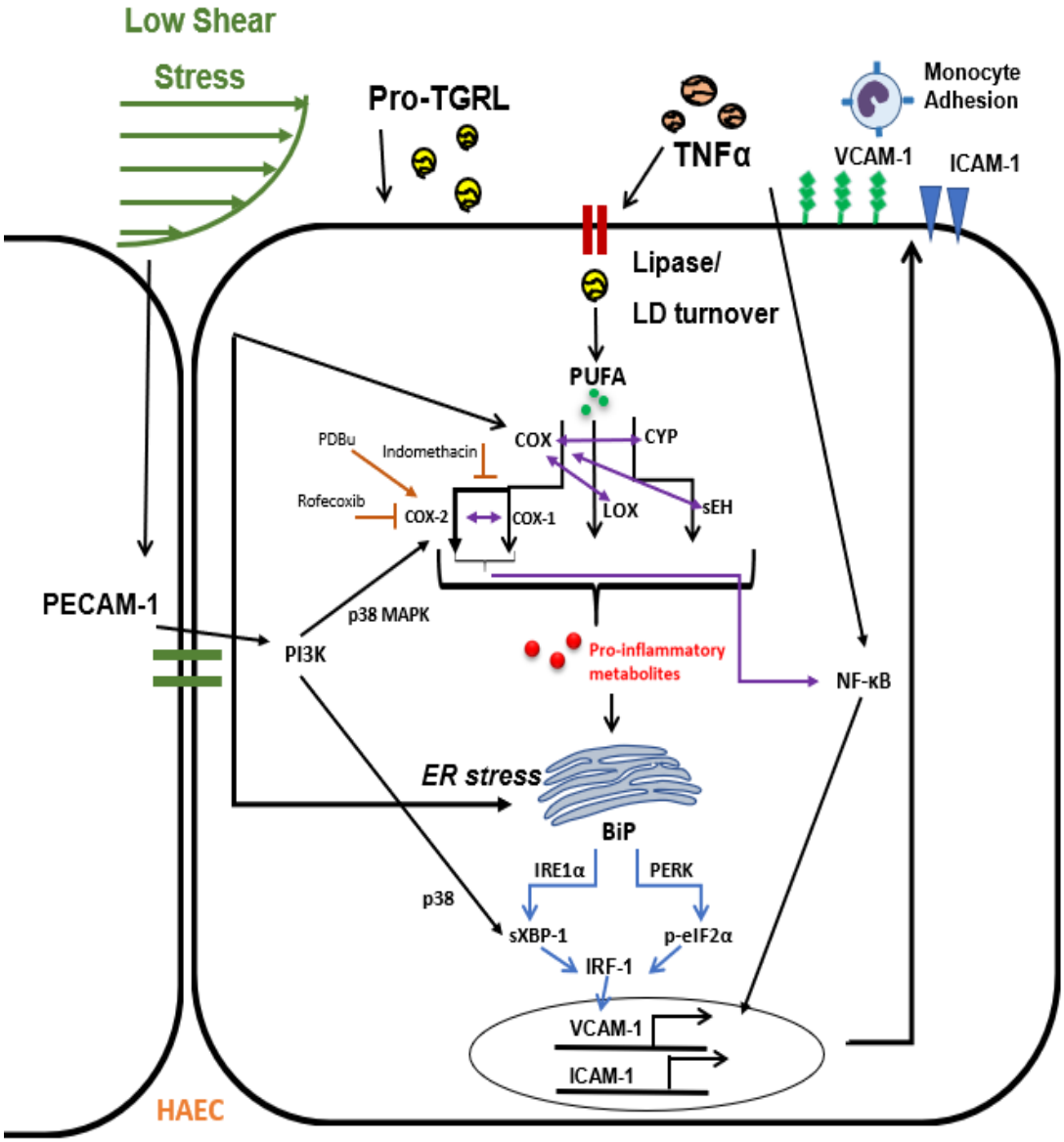

Figure 4.1: HAEC signaling mechanisms model. This illustrates multiple possible pathways in HAEC involving TGRL, COX-2, VCAM-1, and low shear stress. The ER stress response pathway was investigated in this study, but results suggest other mechanisms have an influence on TGRL-induced VCAM-1 response when the COX pathway is manipulated.

CONCLUSION AND FUTURE DIRECTIONS

Conclusion

Modulating the COX-2 pathway, which in turn shifts endothelial PUFA metabolism, altered TGRL-mediated VCAM-1 upregulation, but our results suggest that mechanisms other than those having a direct effect on ER stress may play a more prominent role in mediating the inflammatory response. COX-2 upregulation by pharmacological induction or high magnitude shear stress suppressed ER stress-mediated VCAM-1 elicited by cytokine and lipoprotein by at least 50%. These results are consistent with a protective role for COX-2 in reducing endothelial inflammation that promotes atherosclerosis and suggests low shear stress is more potent than high magnitude shear stress at 12 dynes/cm^2. The study suggests that one way by which low SS can locally promote an atherosusceptible endothelial phenotype is by potently suppressing COX-2 expression to shift fatty acid metabolism away from anti-inflammatory lipid mediators. Ultimately, the potent effect of low SS to promote an atherosusceptible phenotype regardless of COX-2 manipulation demonstrates its crucial importance in models to study athero-inflammation.

By investigating how shear stress modulates the expression of enzymatic pathways connected to the metabolism of fatty acid precursors to bioactive lipids, we expect this project to advance our knowledge of the mechanistic link between nutrition, lipid metabolism, and endothelial mechanobiology in the modulation of athero-inflammation. Understanding these mechanisms will contribute to the lab's long-term goal of being able to accurately link an individual's lipid metabolism with endothelial inflammation to better predict one's susceptibility to atherosclerosis. Ultimately, this project and the recommended future studies could contribute

to the goal of identifying atherosclerotic biomarkers for clinical diagnostics and targets for therapeutic intervention.

Future Directions

Analyses of secreted oxylipin profiles will be essential for future studies to identify the candidate COX-2 metabolites and products of other pathways that mediate the observed pro- and anti-inflammatory responses. Those candidates can be used to assess whether those metabolites alone can shift the inflammatory phenotype to an atheroprotective one. Studies have shown that postprandial anti-TGRL was enriched in non-esterified fatty acids, decreasing IRF-1 expression and consequently VCAM-1 expression. They identified a mechanism by which uptake of lipoproteins sway the inflammatory response of endothelium via VCAM-1.[19] Thus, developing an understanding of how exactly shifting oxylipin profiles in lipoproteins can affect endothelial inflammation to promote early onset atherosclerosis is essential in reducing atherogenesis.

Due to some conflicting results implicating cross talk with other pathways that regulate VCAM-1 expression, further investigation of the effects of COX-2 manipulation on other PUFA metabolic pathways is recommended to fully explain how COX-2 exactly regulates an endothelial inflammatory response. Results suggested that CYP/sEH may be taking on a role in ER-stress mediated VCAM-1 regulation. Thus, the use of dual pharmacological intervention with COX-2 could prove useful to explore crosstalk between the pathways. As mentioned in the discussion, other pathways and signaling mechanisms such as COX-1, LOX, and NF-κB driven pathways are also important to investigate.

Additional recommendations include studying endothelial inflammation and COX-2 expression via the AOC in the presence of anti-inflammatory TGRL. Since shear stress was a potent regulator of inflammation in HAEC exposed to pro-inflammatory TGRL, it is worth investigating its effect with anti-inflammatory TGRL. One important question to address with anti-TGRL would be what the key metabolites are in mediating inflammation, especially in the context of low magnitude shear stress and if induction of those can maintain an anti-inflammatory phenotype under various conditions. It would also be interesting to examine if a linear inverse correlation between VCAM-1 and COX-2 across the shear stress gradient exists in the presence of anti-inflammatory TGRL, as was the case with pro-inflammatory TGRL, or if it would demonstrate a different response. Additionally, anti-inflammatory TGRL used in conjunction with COX-2 pharmacological intervention via western blot and flow cytometry could help elucidate the role of the ER stress mechanism that mediates VCAM-1 regulation.

REFERENCES

1. Tsou, J. K., Gower, R. M., Ting, H. J., Schaff, U. Y., Insana, M. F., Passerini, A. G., & Simon, S. I. (2008). Spatial regulation of inflammation by human aortic endothelial cells in a linear gradient of shear stress. Microcirculation, 15(4), 311-323.

2. DeVerse, J. S., Sandhu, A. S., Mendoza, N., Edwards, C. M., Sun, C., Simon, S. I., & Passerini, A. G. (2013). Shear stress modulates VCAM-1 expression in response to TNF-α and dietary lipids via interferon regulatory factor-1 in cultured endothelium. American Journal of Physiology-Heart and Circulatory Physiology, 305(8), H1149-H1157.

3. Wang, Y. I., Bettaieb, A., Sun, C., DeVerse, J. S., Radecke, C. E., Mathew, S., ... & Simon, S. I. (2013). Triglyceride-rich lipoprotein modulates endothelial vascular cell adhesion molecule (VCAM)-1 expression via differential regulation of endoplasmic reticulum stress. PloS one, 8(10), e78322.

4. Bailey, K. A., Haj, F. G., Simon, S. I., & Passerini, A. G. (2017). Atherosusceptible shear stress activates endoplasmic reticulum stress to promote endothelial inflammation. Scientific reports, 7(1), 1-11.

5. Bailey, K. A., Moreno, E., Haj, F. G., Simon, S. I., & Passerini, A. G. (2019). Mechanoregulation of p38 activity enhances endoplasmic reticulum stress-mediated inflammation by arterial endothelium. The FASEB Journal, 33(11), 12888-12899.

6. Gora, S., Maouche, S., Atout, R., Wanherdrick, K., Lambeau, G., Cambien, F., ... & Karabina, S. A. (2010). Phospholipolyzed LDL induces an inflammatory response in endothelial cells through endoplasmic reticulum stress signaling. The FASEB Journal, 24(9), 3284-3297.

7. Rajamani, A., Borkowski, K., Akre, S., Fernandez, A., Newman, J. W., Simon, S. I., & Passerini, A. G. (2019). Oxylipins in triglyceride-rich lipoproteins of dyslipidemic subjects promote endothelial inflammation following a high fat meal. Scientific reports, 9(1), 1-17.

8. Alexanian, A., & Sorokin, A. (2017). Cyclooxygenase 2: protein-protein interactions and posttranslational modifications. Physiological genomics, 49(11), 667-681.9. Patrono, C. (2016). Cardiovascular effects of cyclooxygenase-2 inhibitors: a mechanistic and clinical perspective. British journal of clinical pharmacology, 82(4), 957-964.

10. Russell-Puleri, S., dela Paz, N. G., Adams, D., Chattopadhyay, M., Cancel, L., Ebong, E., ... & Tarbell, J. M. (2017). Fluid shear stress induces upregulation of COX-2 and PGI2 release in endothelial cells via a pathway involving PECAM-1, PI3K, FAK, and p38. American Journal of Physiology-Heart and Circulatory Physiology, 312(3), H485-H500.

11. Voloshyna, I., Kasselman, L. J., Carsons, S. E., Littlefield, M. J., Gomolin, I. H., De Leon, J., & Reiss, A. B. (2017). COX-2-dependent and independent effects of COX-2 inhibitors and NSAIDs on proatherogenic changes in human monocytes/macrophages. Journal of Investigative Medicine, 65(3), 694-704.

12. Tang, S. Y., Monslow, J., Todd, L., Lawson, J., Puré, E., & FitzGerald, G. A. (2014). Cyclooxygenase-2 in endothelial and vascular smooth muscle cells restrains atherogenesis in hyperlipidemic mice. Circulation, 129(17), 1761-1769.

13. Inoue, H., Taba, Y., Miwa, Y., Yokota, C., Miyagi, M., & Sasaguri, T. (2002). Transcriptional and posttranscriptional regulation of cyclooxygenase-2 expression by fluid shear stress in vascular endothelial cells. Arteriosclerosis, thrombosis, and vascular biology, 22(9), 1415-1420.

14. Chien, S., Li, S., & Shyy, J. Y. (1998). Effects of mechanical forces on signal transduction and gene expression in endothelial cells. Hypertension, 31(1), 162-169.

15. Dogné, J. M., Hanson, J., & Pratico, D. (2005). Thromboxane, prostacyclin and isoprostanes: therapeutic targets in atherogenesis. Trends in pharmacological sciences, 26(12), 639-644.

16. Kawabe, J. I., Ushikubi, F., & Hasebe, N. (2010). Prostacyclin in vascular diseases. Circulation Journal, 1004130682-1004130682.

17. Pahwa R, Jialal I. Atherosclerosis. In: StatPearls. Treasure Island (FL): StatPearls Publishing; 2020.

18. Lin, J. H., Walter, P., & Yen, T. B. (2008). Endoplasmic reticulum stress in disease pathogenesis. Annu. Rev. Pathol. Mech. Dis., 3, 399-425.

19. Sun, C., Alkhoury, K., Wang, Y. I., Foster, G. A., Radecke, C. E., Tam, K., ... & Newman, J. W. (2012). IRF-1 and miRNA126 modulate VCAM-1 expression in response to a high-fat meal. Circulation research, 111(8), 1054-1064.

20. Topper, J. N., Cai, J., Falb, D., & Gimbrone, M. A. (1996). Identification of vascular endothelial genes differentially responsive to fluid mechanical stimuli: cyclooxygenase-2, manganese superoxide dismutase, and endothelial cell nitric oxide synthase are selectively up-regulated by steady laminar shear stress. Proceedings of the National Academy of Sciences, 93(19), 10417-10422.

21. Conway, D. E., Williams, M. R., Eskin, S. G., & McIntire, L. V. (2010). Endothelial cell responses to atheroprone flow are driven by two separate flow components: low time-average

shear stress and fluid flow reversal. American Journal of Physiology-Heart and Circulatory Physiology, 298(2), H367-H374.

22. Gimbrone Jr, M. A., Topper, J. N., Nagel, T., Anderson, K. R., & GARCIA-CARDEÑA, G. U. I. L. L. E. R. M. O. (2000). Endothelial Dysfunction, Hemodynamic Forces, and Atherogenesis a. Annals of the New York Academy of Sciences, 902(1), 230-240.

23. DeVerse, J. S., Bailey, K. A., Foster, G. A., Mittal, V., Altman, S. M., Simon, S. I., & Passerini, A. G. (2012). On-chip endothelial inflammatory phenotyping. JoVE (Journal of Visualized Experiments), (65), e4169.

24. Hernandez, A. A., Foster, G., Fernandez, A., Simon, S., & Singh, G. (2018). CD11c/CD18 Affinity Modulates Monocyte Inflammatory in Primary and Recurrent Myocardial Infarction. Arteriosclerosis, Thrombosis, and Vascular Biology, 38(Suppl_1), A413-A413.

25. Hernandez, A. A., Foster, G. A., Soderberg, S. R., Fernandez, A., Reynolds, M. B., Orser, M. K., ... & Simon, S. I. (2020). An Allosteric Shift in CD11c Affinity Activates a Proatherogenic State in Arrested Intermediate Monocytes. The Journal of Immunology, 205(10), 2806-2820.

26. Parfenova, H., Parfenov, V. N., Shlopov, B. V., Levine, V., Falkos, S., Pourcyrous, M., & Leffler, C. W. (2001). Dynamics of nuclear localization sites for COX-2 in vascular endothelial cells. American Journal of Physiology-Cell Physiology, 281(1), C166-C178.

27. Khyzha, N., Alizada, A., Wilson, M. D., & Fish, J. E. (2017). Epigenetics of atherosclerosis: emerging mechanisms and methods. Trends in molecular medicine, 23(4), 332-347.

28. Nordestgaard, B. G. (2016). Triglyceride-rich lipoproteins and atherosclerotic cardiovascular disease: new insights from epidemiology, genetics, and biology. Circulation research, 118(4), 547-563.

29. Zhou, J., Li, Y. S., & Chien, S. (2014). Shear stress–initiated signaling and its regulation of endothelial function. Arteriosclerosis, thrombosis, and vascular biology, 34(10), 2191-2198.

30. Gimbrone Jr, M. A., & García-Cardeña, G. (2016). Endothelial cell dysfunction and the pathobiology of atherosclerosis. Circulation research, 118(4), 620-636.

31. Cybulsky, M. I., Iiyama, K., Li, H., Zhu, S., Chen, M., Iiyama, M., ... & Milstone, D. S. (2001). A major role for VCAM-1, but not ICAM-1, in early atherosclerosis. The Journal of clinical investigation, 107(10), 1255-1262.

32. Gower, R. M., Wu, H., Foster, G. A., Devaraj, S., Jialal, I., Ballantyne, C. M., ... & Simon, S. I. (2011). CD11c/CD18 expression is upregulated on blood monocytes during hypertriglyceridemia and enhances adhesion to vascular cell adhesion molecule-1. Arteriosclerosis, thrombosis, and vascular biology, 31(1), 160-166.

33. Foster, G. A., Gower, R. M., Stanhope, K. L., Havel, P. J., Simon, S. I., & Armstrong, E. J. (2013). On-chip phenotypic analysis of inflammatory monocytes in atherogenesis and myocardial infarction. Proceedings of the National Academy of Sciences, 110(34), 13944-13949.

34. Shearer, G. C., & Newman, J. W. (2009). Impact of circulating esterified eicosanoids and other oxylipins on endothelial function. Current atherosclerosis reports, 11(6), 403.

35. Das, M., Lu, J., Joseph, M., Aggarwal, R., Kanji, S., McMichael, B. K., ... & Das, H. (2012). Kruppel-like factor 2 (KLF2) regulates monocyte differentiation and functions in mBSA and IL-1β-induced arthritis. Current molecular medicine, 12(2), 113-125.

36. Manoharan, P., Basford, J. E., Pilcher-Roberts, R., Neumann, J., Hui, D. Y., & Lingrel, J. B. (2014). Reduced levels of microRNAs miR-124a and miR-150 are associated with increased proinflammatory mediator expression in Krüppel-like factor 2 (KLF2)-deficient macrophages. Journal of Biological Chemistry, 289(45), 31638-31646.

37. Wang, Y. I., Schulze, J., Raymond, N., Tomita, T., Tam, K., Simon, S. I., & Passerini, A. G. (2011). Endothelial inflammation correlates with subject triglycerides and waist size after a high-fat meal. American Journal of Physiology-Heart and Circulatory Physiology, 300(3), H784-H791.

38. Ting, H. J., Stice, J. P., Schaff, U. Y., Hui, D. Y., Rutledge, J. C., Knowlton, A. A., ... & Simon, S. I. (2007). Triglyceride-rich lipoproteins prime aortic endothelium for an enhanced inflammatory response to tumor necrosis factor-α. Circulation research, 100(3), 381-390.

39. Zhang, H., Li, J., Li, L., Liu, P., Wei, Y., & Qian, Z. (2017). Ceramide enhances COX-2 expression and VSMC contractile hyperreactivity via ER stress signal activation. Vascular pharmacology, 96, 26-32.

40. Jones, R. D., Liao, J., Tong, X., Xu, D., Sun, L., Li, H., & Yang, G. Y. (2019). Epoxy-oxylipins and soluble epoxide hydrolase metabolic pathway as targets for NSAID-induced gastroenteropathy and inflammation-associated carcinogenesis. Frontiers in pharmacology, 10, 731.

41. Norwood, S., Liao, J., Hammock, B. D., & Yang, G. Y. (2010). Epoxyeicosatrienoic acids and soluble epoxide hydrolase: potential therapeutic targets for inflammation and its induced carcinogenesis. American journal of translational research, 2(4), 447.

42. Rand, A. A., Rajamani, A., Kodani, S. D., Harris, T. R., Schlatt, L., Barnych, B., ... & Hammock, B. D. (2019). Epoxyeicosatrienoic acid (EET)-stimulated angiogenesis is mediated by epoxy hydroxyeicosatrienoic acids (EHETs) formed from COX-2. Journal of lipid research, 60(12), 1996-2005.

43. Murata, T., & Maehara, T. (2016). Discovery of anti-inflammatory role of prostaglandin D2. Journal of Veterinary Medical Science, 16-0347.

44. Silverman, M. D., Tumuluri, R. J., Davis, M., Lopez, G., Rosenbaum, J. T., & Lelkes, P. I. (2002). Homocysteine upregulates vascular cell adhesion molecule-1 expression in cultured human aortic endothelial cells and enhances monocyte adhesion. Arteriosclerosis, thrombosis, and vascular biology, 22(4), 587-592.

45. Chen, L., Zhao, Q., Wang, X. L., You, R., Zhang, Y. H., Ji, H., & Lai, Y. S. (2011). ZLJ-6, a novel COX/5-LOX inhibitor, attenuates TNF-α-induced endothelial E-selectin, ICAM-1 and VCAM-1 expression and monocyte–endothelial interactions via a COX/5-LOX-independent mechanism. Vascular pharmacology, 55(5-6), 135-142.

46. Seok, S. M., Park, D. H., Kim, Y. C., Moon, C. H., Jung, Y. S., Baik, E. J., ... & Lee, S. H. (2006). COX-2 is associated with cadmium-induced ICAM-1 expression in cerebrovascular endothelial cells. Toxicology letters, 165(3), 212-220.

47. Park, T. Y., Baik, E. J., & Lee, S. H. (2013). Prostaglandin E2-induced intercellular adhesion molecule-1 expression is mediated by cAMP/Epac signalling modules in bEnd. 3 brain endothelial cells. British journal of pharmacology, 169(3), 604-618.

48. Uehara, Y., Murata, Y., Shiga, S., & Hosoi, Y. (2016). NSAIDs diclofenac, indomethacin, and meloxicam highly upregulate expression of ICAM-1 and COX-2 induced by X-irradiation in human endothelial cells. Biochemical and biophysical research communications, 479(4), 847-852.

49. Simion, V., Zhou, H., Pierce, J. B., Yang, D., Haemmig, S., Tesmenitsky, Y., ... & Feinberg, M. W. (2020). LncRNA VINAS regulates atherosclerosis by modulating NF-κB and MAPK signaling. JCI insight, 5(21).

50. Huang, W. C., Wu, L. Y., Hu, S., & Wu, S. J. (2018). Spilanthol Inhibits COX-2 and ICAM-1 expression via suppression of NF-κB and MAPK signaling in interleukin-1β-stimulated human lung epithelial cells. Inflammation, 41(5), 1934-1944.

51. Onodera, Y., Teramura, T., Takehara, T., Shigi, K., & Fukuda, K. (2015). Reactive oxygen species induce Cox-2 expression via TAK1 activation in synovial fibroblast cells. FEBS open bio, 5, 492-501.

52. Hussain, A., Ballantyne, C. M., Saeed, A., & Virani, S. S. (2020). Triglycerides and ASCVD risk reduction: recent insights and future directions. Current Atherosclerosis Reports, 22, 1-10.

53. Schwartz, E. A., & Reaven, P. D. (2012). Lipolysis of triglyceride-rich lipoproteins, vascular inflammation, and atherosclerosis. Biochimica et Biophysica Acta (BBA)-Molecular and Cell Biology of Lipids, 1821(5), 858-866.